

Fig. 1. Kinetics of γ H2AX foci formation/disappearance in G_0/G_1 human cells irradiated with 1 Gy of X-rays and carbon ions (linear energy transfer, 13 and 70 keV/ μ m).

human cells in G_0/G_1 phases with 1 Gy of X-rays and carbon ions (290 MeV/u). Two LET values, 13 and 70 keV/ μ m, were used for carbon-ion experiments. The focus kinetics for X-rays and low-LET carbon ions (13 keV/ μ m) revealed efficient disappearance of the foci. In contrast, the focus kinetics for high-LET carbon ions (70 keV/ μ m) showed inefficient focus disappearance, leading to more cell killing when compared to low-LET irradiation cases. Since 13 keV/ μ m is the LET for the flat portion of the SOBP for carbon-ion beam, our data help explain the successful carbon-ion treatment outcome; a tumor mass can be targeted with the high-LET portion (e.g., 70 keV/ μ m), and surrounding normal tissue can be spared with the low-LET portion (13 keV/ μ m). These γ H2AX data seem to substantiate the data obtained by the traditional gel-based assay.

Effect of high-LET heavy ions at the chromosome level

The DNA DSB repair results described in Fig. 1 should be reflected at the chromosome level as the remaining DSBs that could be converted into chromosome aberrations. Here the results with the premature chromosome condensation (PCC) assay are mentioned to determine the early post-irradiation behavior of cells. Prematurely condensed chromosomes can be obtained by fusing interphase cells such as cells in G_1 or G_2 phase with mitotic cells using facilitating agents such as Sendai virus or polyethylene glycol. By fusing these cells, factor(s) to condense chromosomes would be transferred from mitotic to interphase cells, and condensed interphase chromosomes can be observed.⁶⁸⁻⁷¹ By this method, kinetics of chromosome-break rejoining can be measured at comparatively low doses (< 5 Gy). Furthermore, if one combines the PCC assay with fluorescence *in situ* hybridization (FISH), information on mis-rejoined chromosomes can be obtained. Our data from these measurements using irradiated primary human cells at G_0/G_1 phases are shown in Table 1. Regarding the data in Table 1, chromosomes 1 and 2 are stained by individual whole chromosome painting probes; "fragment" means an isolated stained chro-

Table 1. Frequency of chromosome aberrations in G_1 phase human cells irradiated with 2 Gy of X-rays, carbon (linear energy transfer [LET], 13 and 70 keV/ μ m) and iron (200 keV/ μ m) ions as measured by the premature chromosome condensation and fluorescence *in situ* hybridization technique, where 50-70 cells were scored for each radiation type.

Radiation type	LET (keV/ μ m)	Exchange frequency	Fragment frequency
X-rays	2	0.23	0.16
Carbon ions	13	0.40	0.37
	70	0.45	0.71
Iron ions	200	0.61	0.88

matid shorter than the original unbroken chromatid, and "exchange" indicates chromatid partially stained with the probe. LET-dependent increases can be observed in these aberrations, and this is more true in the frequency of fragments, while there is a much smaller increase in the frequency of exchanges as a function of LET. For example, the exchange rate at 13 keV/ μ m is not much different from that at 70 keV/ μ m, suggesting that high-LET radiation may induce more chromosome breaks than exchanges.

Gene expression after high-LET heavy ions differs from that after X-rays

At NIRS, a unique gene expression analysis method called HiCEP (high coverage expression profiling) was developed. Although more effort and resources may be needed to obtain the expression data with HiCEP when compared with other assays such as microarray, this method can provide more accurate and reproducible results with a great sensitivity.^{72,73} Genes not previously identified after a specific damaging agent could be uncovered.⁷⁴ In our recent HiCEP experiment with normal human cells, differences were observed when the profile obtained with high-LET car-

bon ions (70 keV/ μm) was compared to that with X-rays or low-LET carbon ions (13 keV/ μm). For example, *ATF3* (activating transcription factor 3) gene was significantly upregulated after both high- and low-LET radiation at 2 h post-irradiation, while at 6 h post-irradiation this gene remained at a high level only with high-LET irradiation (A. Fujimori and R. Okayasu, personal communication). Thus, it is evident that the cellular response to high-LET radiation is different from that to low-LET radiation at the gene expression level.

Variation in cell survival levels throughout the cell cycle is reduced in mammalian cells exposed to high-LET radiation

The variation in radiosensitivity throughout the cell cycle has been known for a long time in the case of low-LET radiation in mammalian cells. In general, mitotic cells are most radiosensitive and late S-phase cells are most radioresistant; cells with a long G₁ phase can have another radioresistant peak in G₁.¹⁰ With high-LET irradiation, this may not be the case. In 1975 in Berkeley, USA, using an accelerator, Bird and Burki showed an LET-dependent variation in radiosensitivity as a function of the cell cycle phase in hamster cells.⁷⁵ With increasing LET (up to ~200 keV/ μm), the variation throughout the cell cycle was significantly reduced; there was very little variation as LET reached about 200 keV/ μm . Although that work was very significant, cell cycle work with high-LET radiation has not been repeated until very recently.⁷⁶ At HIMAC, we have repeated experiments similar to those at Berkeley using Chinese hamster ovary (CHO) cells. We also found that the cell survival variation throughout the cell cycle became much less with 70 keV/ μm carbon-ion irradiation, and this was further reduced with 200 keV/ μm iron ions. Moreover, using two types of DNA DSB repair deficient CHO mutants, we found that the cause of such reduced variation in radiosensitivity may stem from the inhibition/reduction of both non-homologous end-joining and homologous recombination repair as a consequence of complex DNA damage induced by high-LET radiation.⁷⁰ Further detailed studies on this subject are currently underway in our laboratory.

Conclusion

Here we emphasized the importance of DNA DSB repair induced by high-LET radiation. If DSB repair is inefficient with high-LET heavy ions, this leads to chromosome damage and eventually cell killing. Since the DNA damage induced by high-LET radiation is different from that by low-LET radiation, different mechanisms to repair DNA damage by high-LET radiation might be necessary. This could contribute to the elucidation of a novel DNA damage repair pathway. Heavy-ion facilities such as HIMAC may prove to be very useful for the investigation of fundamental cell biology, in addition to their proven clinical benefit.

RADIOBIOLOGICAL SIGNIFICANCE OF THE SENSITIVITY AND RECOVERY FOLLOWING EXPOSURE TO ACCELERATED CARBON-ION BEAMS COMPARED WITH γ -RAYS, WITH REFERENCE TO THOSE IN INTRATUMOR QUIESCENT CELLS

Background

Human solid tumors are thought to contain moderately large fractions of quiescent (Q) tumor cells, which are out of the cell cycle and stop cell division, but they are as viable as established experimental animal tumor lines that have been employed for various oncology studies.⁷⁷ The presence of Q cells is probably due, at least in part, to hypoxia and the depletion of nutrition in the tumor core, a consequence of poor vascular supply.⁷⁷ As a result, Q cells are viable and clonogenic, but cell division has ceased. In general, radiation and many DNA-damaging chemotherapeutic agents kill proliferating (P) tumor cells more efficiently than Q tumor cells, resulting in many clonogenic Q cells remaining following radiotherapy and chemotherapy.⁷⁷ Therefore, it is harder to control Q tumor cells than to control P tumor cells, and many post-radiotherapy recurrent tumors result partly from the regrowth of Q tumor cell populations that could not be sufficiently killed by radiotherapy.⁷⁷ Further, sufficient doses of drugs cannot be distributed within Q tumor cell populations mainly due to the heterogeneous and poor vascular distributions within solid tumors. Thus, one of the major causes of post-chemotherapy recurrent tumors is an insufficient dose distribution in Q cell fractions.⁷⁸

Meanwhile, high-LET radiation provides higher RBE for cell killing, reduced oxygen effect, and reduced dependence on the cell cycle,¹² making it potentially superior to low-LET radiation in the treatment of malignant tumors. Therefore, using our method for selectively detecting the response of Q cells within solid tumors,³⁹ we have examined the characteristics of radiosensitivity in total (= P + Q) and Q cell populations in solid tumors irradiated with carbon ions at various LET values in a 6-cm SOBP compared to those irradiated with ⁶⁰Co γ -rays and reactor thermal and epithermal neutrons at the Kyoto University Research Reactor Institute. Further, we have examined the effect of the post-irradiation oxygenation status on recovery from radiation-induced damage in total and Q cell populations in solid tumors *in vivo* after low-LET γ -ray and carbon-ion irradiation. In addition, in the future, we will analyze the relationship between the depth within the SOBP and the value of RBE based on the sensitivity of Q tumor cells, and further optimize carbon-ion therapy.

Method for selectively detecting the response of Q cells in solid tumors to DNA-damaging treatment

Using asynchronous tumor cell cultures and cell cultures

blocked for a short time with an S phase cell toxin, hydroxyurea, the cell-survival curve, which cannot be obtained directly by routine colony formation assay, can be calculated using the micronucleus (MN) frequency and the regression line between the surviving fraction and MN frequency for asynchronous cell cultures.⁷⁹⁾ Therefore, it was thought to be possible to detect the response of Q cells in solid tumors using immunofluorescence staining for 5-bromo-2'-deoxyuridine (BrdU) and the MN assay following continuous BrdU labeling of intratumor P cells.

Tumor-bearing mice received various DNA-damaging treatments after 10 injections of BrdU at 12-h intervals or continuous administration of BrdU to label all P cells in solid tumors. The tumors were then excised and trypsinized. The obtained tumor cell suspensions were incubated with a cytokinesis blocker cytochalasin-B for 48–72 h, and the MN frequency in these cells without BrdU labeling was determined using immunofluorescence staining for BrdU. This MN frequency was then used to determine the surviving fraction of the BrdU-unlabeled cells from the regression line obtained between the MN frequency and the surviving fraction determined for total cells in the tumor. Thus, a cell-survival curve could be determined for cells not labeled by BrdU, which could be regarded for all practical purposes as Q cells in a solid tumor.⁸⁰⁾ Incidentally, the apoptosis frequency instead of the MN frequency was also shown to be applicable to this method.³⁹⁾

Demonstrated characteristics of quiescent cells in solid tumors

Using our method after low-LET irradiation of tumor-bearing mice, the following characteristics of Q cells in murine solid tumors were clarified: Q tumor cells are more radioresistant than total (P + Q) tumor cells; Q cells have greater potentially lethal damage repair (PLDR) capacity than total cells; and Q cell populations include a higher hypoxic fraction (HF) than total cells.⁸⁰⁾ It was also indicated that the clonogenicity of Q cells is lower than that of P cells, and that the HF of Q cells is largely comprised of chronically HF with a smaller proportion of acutely HF. Concerning the *p53* status of tumor cells, SAS/*mp53* tumors (which harbor mutated *p53*) include a larger size of not only HF but also chronically HF than SAS/*neo* tumors (which harbor normal *p53*), and Q cell populations in both tumors include higher HF, particularly chronically HF, than total cell populations, especially in regard to SAS/*neo* tumors.³⁹⁾

Meanwhile, when the solid tumors were irradiated with high-LET fast neutrons or reactor neutrons, the difference in intrinsic radiosensitivity between total tumor and Q cells was markedly reduced, compared with low-LET photons, especially at high radiation doses.^{81,82)} As for neutron capture reaction with ¹⁰B-compounds, *L-para*-boronophenylalanine (BPA) increased the sensitivity of the total cells more than sodium mercaptoundecahydro (BSH). However, BPA-treated

Q cells were less sensitive than BSH-treated Q cells. The difference in sensitivity between total and Q cells was greater with ¹⁰B-compounds, especially BPA.⁸²⁾ Q cells showed greater PLDR capacity than total cells. γ -Ray irradiation and neutron irradiation with BPA induced greater PLDR capacity in both cell populations. In contrast, thermal neutron irradiation without the ¹⁰B-compound induced the smallest PLDR capacity in both. The use of the ¹⁰B-compound, especially BPA, increased the PLDR capacity in both cell populations, and made the PLDR patterns of both look like those induced by γ -ray irradiation.⁸³⁾ In both total and Q tumor cells, HF increased immediately after neutron irradiation. Reoxygenation after each neutron irradiation occurred more rapidly in total cells than in Q cells. In both cell populations, reoxygenation appeared to be rapidly induced in the following order: neutron irradiation without ¹⁰B-compounds > neutron irradiation following BSH injection > neutron irradiation following BPA administration > γ -ray irradiation.⁸⁴⁾

Response of total and quiescent tumor cells in vivo to carbon ions compared with γ -rays and reactor neutrons

SCC VII tumor-bearing mice were continuously given BrdU to label all intratumor P cells. Then, they received carbon ions or γ -rays at a high dose rate (HDR, 1.0–2.0 Gy/min) or reduced dose rate (RDR, 0.035–0.040 Gy/min). Other tumor-bearing mice received reactor thermal or epithermal neutrons at RDR. Immediately after HDR and RDR irradiation and 12 h after HDR irradiation, the response of Q cells was assessed for MN frequency using immunofluorescence staining for BrdU. The response of total (= P + Q) tumor cells was determined from the BrdU non-treated tumors.

The difference in radiosensitivity between total and Q cell populations under γ -ray irradiation was markedly reduced with reactor neutrons and carbon ions, especially at higher LET, which is available at a deeper point within SOBP of carbon ions. More pronounced repair in Q cells than total cells through a delayed assay or a decrease in dose rate under γ -ray irradiation was efficiently inhibited with carbon ions, especially at higher LET. Under RDR irradiation, the radiosensitivity to high-LET carbon ions was quite similar to that to reactor thermal and epithermal neutrons (Fig. 2). In terms of tumor cell-killing effect as a whole, including Q tumor cells, carbon ions, especially at higher LET, are very useful for suppressing dependence on the heterogeneity within solid tumors as well as depositing radiation dose precisely.^{38,85)}

Relationship between post-irradiation tumor oxygenation status and radiosensitivity of irradiated tumors in vivo

BrdU-labeled SCC VII tumor-bearing mice received γ -

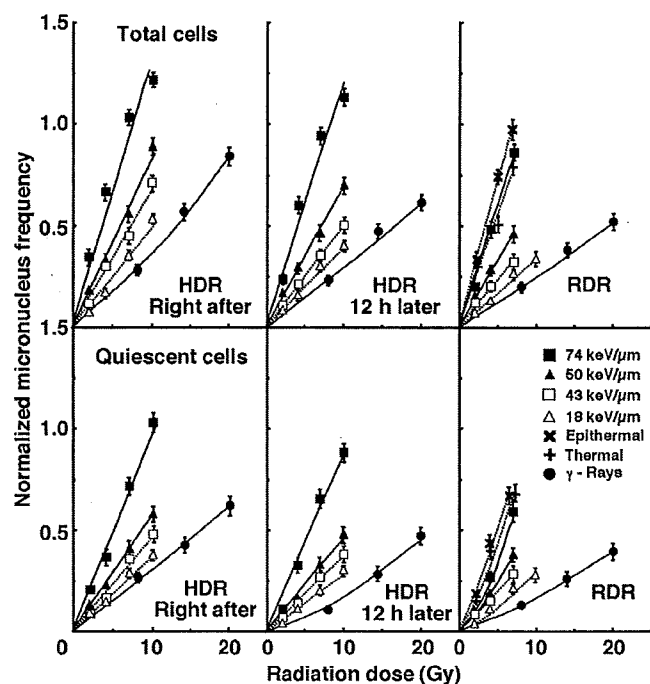


Fig. 2. Dose-response curve of normalized micronucleus frequency for total (upper panel) and quiescent (lower panel) tumor cell populations as a function of radiation dose immediately after high dose-rate (HDR) irradiation, 12 h after HDR irradiation, and immediately after reduced dose-rate (RDR) irradiation are shown in the left, middle, and right panel, respectively. Open triangles, open squares, solid triangles, and solid squares represent the normalized micronucleus frequency after carbon-ion irradiation at linear energy transfer of 18, 43, 50 and 74 keV/μm, respectively. Solid circles represent the data after γ -ray irradiation. The cross and X-shaped symbols represent the data after reactor thermal and epithermal neutron irradiation, respectively. Bars represent standard error.

rays or carbon ions with or without tumor clamping to induce hypoxia. Immediately after irradiation, cells from some tumors were isolated, or acute hypoxia-releasing nicotinamide was loaded to the tumor-bearing mice. For 9 h after irradiation, some tumors were kept aerobic or hypoxic. Then, isolated tumor cells were incubated with a cytokinesis blocker. Finally, the response of Q and total tumor cells was assessed for MN.

Inhibition of recovery from radiation-induced damage by keeping irradiated tumors hypoxic after irradiation and promotion of recovery by nicotinamide loading were observed more clearly with γ -rays, after aerobic irradiation and in total cells than with carbon ions, after hypoxic irradiation and in Q cells, respectively (Fig. 3). The tumor oxygenation status following irradiation can influence recovery from radiation-induced damage, especially after aerobic γ -ray irradiation in total cells. In other words, the tumor oxygenation status not only during irradiation but also after irradiation can affect

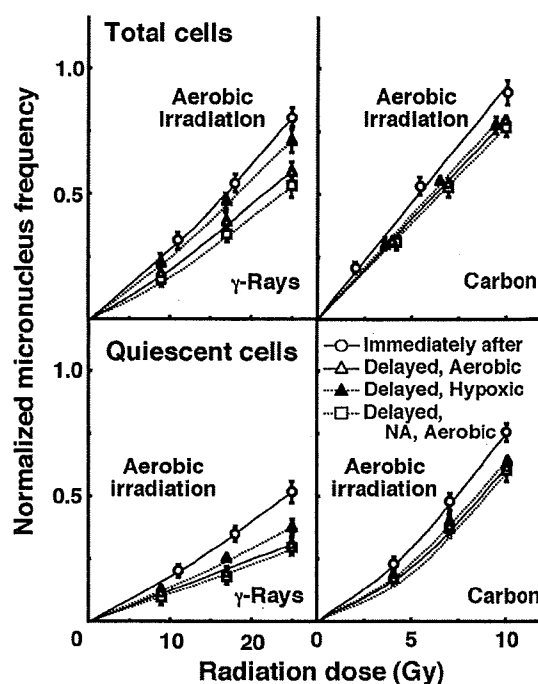


Fig. 3. Dose response curve of normalized micronucleus frequency for total (upper panel) and quiescent (lower panel) tumor cells as a function of dose immediately and 9 h after irradiation. The data after γ -ray and carbon-ion irradiation are shown in the left and right panels, respectively. The data after irradiation under aerobic condition are shown. Open circles, open triangles, solid triangles, and open squares represent the data immediately after irradiation, after keeping tumors aerobic for 9 h following irradiation, after keeping tumors hypoxic for 9 h following irradiation, and after keeping tumors aerobic for 9 h following the administration of nicotinamide (NA) immediately after irradiation, respectively. Bars represent standard error.

the radiosensitivity of solid tumors, and especially with γ -rays. In this respect, carbon ions are promising because of their efficient suppression of recovery almost independently of the tumor oxygenation status.⁸⁶⁾

Carbon ions – conclusion

In terms of the tumor cell-killing effect as a whole, including intratumor Q cell control, carbon-ion therapy can be a very promising treatment modality for deep-seated refractory tumors because of its very efficient cytotoxic effect on intratumor Q cell populations particularly at a deeper point within SOBP of carbon ions, taking into account the very advantageous potential of depositing the radiation dose very precisely using SOBP.³⁸⁾ Further, in both total and Q tumor cells, carbon-ion irradiation is less dependent on the oxygen condition at the time of irradiation, with little or no recovery from radiation-induced DNA damage, as well as being without dependence on the post-irradiation intratumor oxygenation status, thus leading to higher RBE

compared with γ -ray irradiation.⁸⁶⁾

***p53*-INDEPENDENT APOPTOSIS IS A POTENTIAL TARGET FOR HIGH-LET HEAVY-ION THERAPY**

Background

The evaluation of biological markers is of interest in view of their potential ability to predict the outcome of cancer therapy. It has been reported that *p53* mutations and deletions occur in many advanced human cancers,⁸⁷⁾ and lead to resistance to X-rays^{44-46,88,89)} used for cancer therapy (Fig. 4a). Thus the genetic and functional *p53* status may be important in guiding therapeutic strategy for cancer patients.⁹⁰⁾ The *p53* protein has multiple functional activities, (e.g., as a sequence-specific transcription factor whose transcriptional target genes induce growth arrest and apoptosis).⁹¹⁾ In mutated *p53* (*mp53*) tumors, resistance to radiotherapy may result from failure to induce apoptosis, because X-rays kill cancer cells partly *via* apoptosis. The involvement of *p53* in the sensitivity of many cell types to low-LET radiation is well established.

As discussed in the Introduction, high-LET heavy ions have several potential advantages over photons: (i) excellent dose distribution, (ii) high RBE, (iii) reduction in oxygen enhancement ratio, (iv) little variation in cell cycle-related radiosensitivity, and (v) small influence from radiation repair process. The spatial distribution of nuclear DNA lesions produced by charged particles depends on the ion track structure.⁹²⁾ As a result, high-LET heavy ions have highly lethal effects, even on radioresistant tumors. It is conceivable that effective therapeutic strategies may be designed based on the genetic and biochemical events involved in cell death. Therefore, accurate characterization and quantification of the process by which radiation leads to cell death (e.g., apoptosis and necrosis) have become increasingly important in further understanding the biological effectiveness of high-LET radiation. Currently, little information is available on the relationship between *p53* status in tumor cells and on the ability to undergo apoptosis after high-LET irradiation. However, work has been done in this area, and some basic studies are reviewed here concerning the possibility that *p53*-independent apoptosis offers an effective target for high-LET heavy-ion therapy.

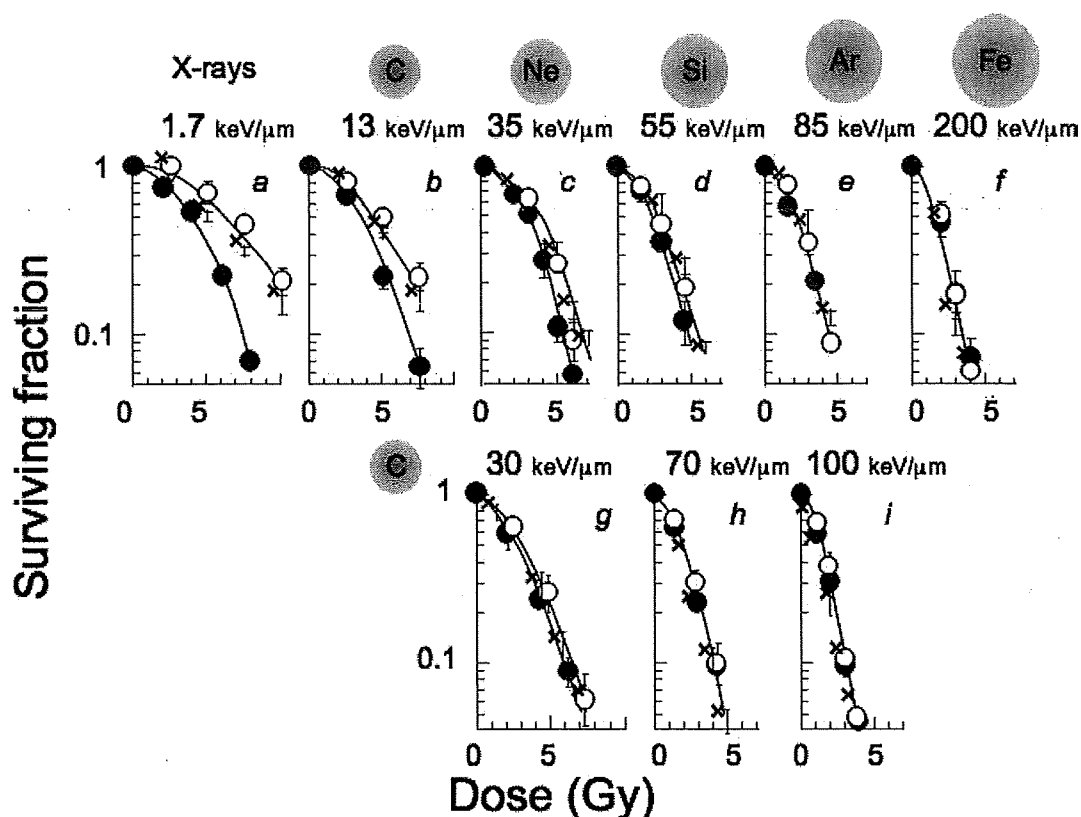


Fig. 4. Survival curve for cultured human lung cancer cells.^{93,94)} Panel *a*, X-rays (200 kVp, 1.7 keV/μm); *b*, carbon (290 MeV/u, 13 keV/μm); *c*, neon (400 MeV/u, 35 keV/μm); *d*, silicon (490 MeV/u, 55 keV/μm); *e*, argon (500 MeV/u, 85 keV/μm); *f*, iron (500 MeV/u, 200 keV/μm); *g*, carbon (290 MeV/u, 30 keV/μm); *h*, carbon (290 MeV/u, 70 keV/μm); *i*, carbon (290 MeV/u, 100 keV/μm) ions. x, *p53*-null cells; ○, *mp53* cells; ●, *wtp53* cells. Error bars indicate standard deviation.

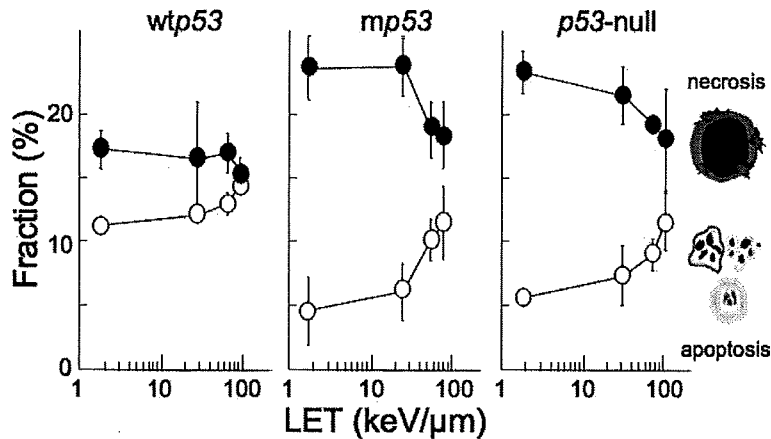


Fig. 5. Radiation-induced apoptosis and necrosis dependence on linear energy transfer (LET).⁹⁴ Cells were cultured in normal medium for 48 h after irradiation with a 30% survival dose and analyzed by acridine orange/ethidium bromide staining method. ○, apoptotic cells; ●, necrotic cells. Error bars indicate standard deviation.

Survival after exposure to different heavy-ion beams

Wild-type (wt) *p53*, *mp53* and *p53*-null cell lines used were derived from H1299 human lung cancer cell line that is *p53*-null. At HIMAC or NIRS, cells were exposed to different types of heavy ions, such as carbon (energy, 290 MeV/u; LET, 13 keV/μm), neon (400 MeV/u, 35 keV/μm), silicon (490 MeV/u, 55 keV/μm), argon (500 MeV/u, 85 keV/μm) and iron (500 MeV/u, 200 keV/μm) ions (Fig. 4b–f). Cellular radiosensitivity was determined using the colony formation assay. It was observed that *wtp53* cells were about 1.6-fold more sensitive to X-rays than the other cell lines (Fig. 4e and f).⁹³ However, it is still unclear which factor affects *p53*-independent radiosensitivity: ion species or LET.

Survival after exposure to carbon ions at different LET

Using polymethyl methacrylate or plastic film absorbers, cellular sensitivity to 290 MeV/u carbon ions at different LET (13, 30, 70 and 100 keV/μm) was examined (Fig. 4b, g–i). As LET increased up to 100 keV/μm, there was almost no significant difference in survival among the cell lines (Fig. 4h and i).⁹⁴ Thus, the range of LET, but not ion species, appears to determine *p53*-independent radiosensitivity.

LET dependence of radiation-induced apoptosis and necrosis

Cell death through apoptosis and necrosis was evaluated with acridine orange (AO)/ethidium bromide (EB) double staining for fluorescence microscopy. This method employs the differential uptake of the fluorescent DNA binding dyes AO and EB, allows morphologic visualization of chromatin condensation in the stained nucleus, and permits distinguishing viable, apoptotic, and necrotic cells. Apoptosis increased with increasing LET, even at isosurvival doses among cell lines (Fig. 5).⁹⁴ These results also agree well with a previous

report using *p53*-deficient human lymphoblastoid cells⁹⁵ and Chinese hamster cells bearing an *mp53* gene.⁹⁶ It was suggested that high-LET radiation might induce not only *p53*-dependent apoptosis but also *p53*-independent apoptosis, resulting in much more severe DNA damage than low-LET radiation. The fact that the surviving fraction after high-LET irradiation was almost the same among *wtp53*, *mp53*, and *p53*-null cells suggests that these cells may die through *p53*-independent pathways. Therefore, radiotherapy with high-LET radiation is certainly of interest as a modality in interdisciplinary cancer therapy regardless of the cellular *p53* status.

p53-independent apoptosis pathways

Caspases serve as the main effectors of apoptosis. Two distinct pathways upstream of the caspase cascade have been identified: death receptor-induced apoptosis and mitochondrial stress-induced apoptosis. Death receptors (e.g., CD95/APO-1/Fas, TNF-R, TRAIL-R) trigger caspase-8, and the mitochondria subsequently release apoptogenic factors (cytochrome *c*, Apaf-1, AIF), leading to the activation of caspase-9.³⁶ Although the two pathways are intimately connected, any cross-communication or crosstalk is minimal, and the two pathways operate largely independently of each other. The caspase systems remain largely unknown in *p53*-independent apoptosis after high-LET irradiation. Human gingival cancer cells (Ca9-22 cells) containing *mp53* gene also showed high sensitivity to high-LET radiation with high apoptotic frequency.⁹⁷ Caspase-3 activity was analyzed by Western blotting and flow cytometry. Caspase 3 was cleaved and activated upon high-LET irradiation, leading to cleavage of poly (ADP-ribose) polymerase.⁹⁷ In addition, caspase-9 inhibitor suppressed caspase-3 activation and apoptosis induction resulting from high-LET radiation to a greater

extent than caspase-8 inhibitor.⁹⁷⁾ These results suggest that caspase-9 may contribute to caspase-dependent apoptosis after high-LET irradiation, i.e., high-LET radiation may activate the mitochondrial-associated apoptotic pathway in a *p53*-independent manner.³⁶⁾ Apoptotic pathways triggered by high-LET radiation do not require *p53*. Severe damage induced by high-LET radiation acts as a trigger for activation of the caspase-9-related apoptotic pathway, rather than the caspase-8 apoptotic pathway. After caspase-9 activation by high-LET radiation, caspase 3 is activated by caspase-9, and this leads to *p53*-independent apoptosis. In this situation, caspase 8 would not be activated because *p53* is defective and not functional, and activation of the death receptor pathways would make minor contributions to apoptosis induction.

High-LET radiation can induce apoptosis effectively regardless of the *p53* status. Thus, cells exposed to high-LET radiation appear to enter apoptosis through the action of downstream effectors of *p53*-centered signal transduction pathways, regardless of the presence or absence of functional *p53*. The question of whether high-LET radiation triggers the mitochondrial apoptosis pathway directly or activates upstream effectors of the mitochondrial pathway remains to be addressed. Further studies should provide new insights into high-LET radiation-enhanced apoptosis, observed to occur in response to selective activation of the mitochondrial apoptotic factor caspase 9 in a *p53*-independent manner.

Prospective views

These findings suggest that high-LET heavy-ion therapy would be a valid application for patients harboring *mp53* and *p53*-null cancer cells. In addition, an advanced charged particle therapy for cancer should be a human-friendly therapy that places fewer physical burdens on patients. However, because of the prohibitive cost and huge accelerator size, there are as yet only a few heavy-ion therapy facilities in the world. Consequently, at present, not many cancer patients can receive heavy-ion therapy. For future investigation, it is proposed that the elucidation of *p53*-independent apoptosis-related genes could provide new insights into cancer radiotherapy that can be used regardless of *p53* status (Fig. 6). Therefore, it is important to characterize these radiation-regulated genes and pathways in heavy ion-irradiated cells, and to elucidate the regulatory mechanisms involved in the expression of these genes.

BCL-2 AS A POTENTIAL TARGET FOR HEAVY-ION THERAPY

As mentioned in the previous section, genetic changes that accompany cancer development and progression endow tumor cells with a survival advantage over their normal counterparts, often leading to a poor prognosis because of resistance to a multitude of therapeutic modalities. Of these,

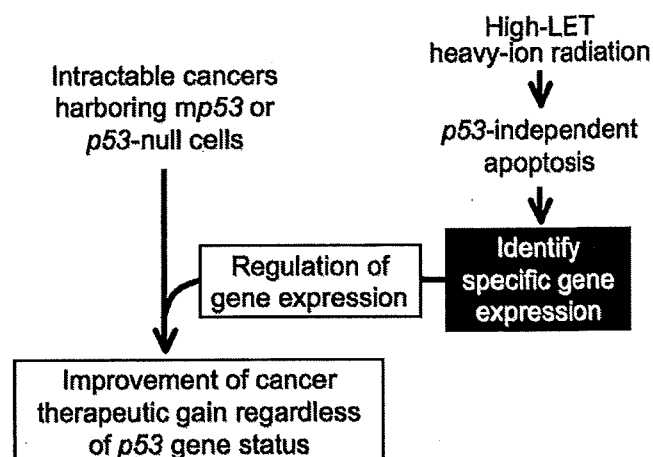


Fig. 6. Strategy for improving cancer therapy regardless of *p53* status. LET, linear energy transfer.

Bcl-2 is an anti-apoptotic protein initially identified as an oncogene in follicular B-cell lymphoma where the t(14;18) chromosomal translocation results in constitutive upregulation of *Bcl-2* expression.^{98,99)} *Bcl-2* overexpression occurs in the tumors of 35–50% of cancer patients; for instance, *Bcl-2* is overexpressed in 50–100% of colorectal cancer, 60–80% of breast cancer, 60–80% of small cell lung cancer, and 65% of melanoma.^{99,100)} Significant evidence has accumulated that *Bcl-2* overexpression has been associated with resistance to conventional photons and chemotherapeutic agents.^{99–101)} Restoring susceptibility by nullifying the effects of *Bcl-2* would hence be an attractive strategy to improve therapeutic efficacy. Despite a series of studies having focused on tumor sensitization to photons by chemical and antisense-based *Bcl-2* inhibitors,^{100–102)} the potential impact of heavy ions on *Bcl-2* overexpressing tumors remains uncharacterized. To address this, we used *Bcl-2* cells (human cervical cancer-derived HeLa cells stably overexpressing *Bcl-2*) and Neo cells (neomycin resistant gene-expressing HeLa cells), with the former expressing nine-fold higher levels of *Bcl-2* proteins than the latter.^{26,102,103)}

At first, the effect of heavy-ion irradiation alone was examined.³⁷⁾ Colony formation assay revealed that, while *Bcl-2* cells were more resistant to ⁶⁰Co γ -rays (LET, 0.2 keV/ μ m) and helium ions (energy, 12.5 MeV/u; LET, 16.2 keV/ μ m) than Neo cells, exposure to five different types of heavy ions (76.3–1610 keV/ μ m) yielded similar clonogenic survival regardless of *Bcl-2* overexpression.³⁷⁾ Terminal deoxynucleotidyl transferase-mediated dUTP-biotin nick-end labeling assay showed that irradiation with carbon ions (18.3 MeV/u, 108 keV/ μ m), which gave maximum RBE for survival, enhanced the apoptotic response of *Bcl-2* cells and decreased the difference in apoptotic incidence between *Bcl-2* and Neo cells.³⁷⁾ Flow cytometric analysis demonstrated

that, unlike the case for γ -rays, carbon-ion exposure prolonged G₂/M arrest, and it occurred more extensively in Bcl-2 cells than in Neo cells.³⁷⁾ Our preliminary data obtained with the Western blot analysis illustrated that whereas exposure to either carbon ions or γ -rays fails to alter the amount of Bcl-2 proteins, the former augments Bcl-2 phosphorylation at serine 70 more effectively than the latter (unpublished data), warranting further studies to delineate the intermediate molecular events. Collectively, these results indicate that high-LET heavy ions overcome tumor radioresistance caused by *Bcl-2* overexpression, which might be potentially accounted for at least in part by the enhanced apoptotic response and prolonged G₂/M arrest. Thus, heavy-ion therapy may be a promising modality for *Bcl-2* overexpressing radioresistant tumors. Moreover, noteworthy is not merely the fact that *Bcl-2* overexpression (and *p53* mutations as reviewed in the previous section) arises in nearly half of human cancers and is related to radioresistance and chemoresistance,^{99,100,104)} but also that such radioresistance can be overcome with heavy ions.^{36,37)} Heavy ions thence appear to effectively inactivate a wide variety of radioresistant tumors, and possibly chemoresistant tumors as well.

Secondly, the combinational effect of Bcl-2 inhibitor and heavy ions was assessed.⁴¹⁾ Ethyl 2-amino-6-bromo-4-(1-cyano-2-ethoxy-2-oxoethyl)-4H-chromene-3-carboxylate (HA14-1) is a novel Bcl-2 inhibitor recently identified from *in silico* screening, and is a nonpeptidic small-molecule ligand (molecular weight = 409) of a Bcl-2 surface pocket.¹⁰⁵⁾ Mounting evidence has indicated that HA14-1 selectively disturbs the interaction between Bcl-2 and Bax and sensitizes tumors to photons.^{106,107)} On the one hand, colony formation assay showed little difference in the cytotoxicity of HA14-1 to Bcl-2 cells and Neo cells, such that its 1-h treatment at 15 μ M resulted in a surviving fraction of 58% for both cell types.⁴¹⁾ Compared with irradiation alone, pre-irradiation treatment for 1 h with 15 μ M HA14-1 potentiated killing of Bcl-2 and Neo cells by carbon ions and γ -rays.⁴¹⁾ On the other hand, it would be desirable if a radiosensitizer could exert cytotoxic and sensitizing effects preferentially to tumors with minimal adverse effects to normal cells, and this was therefore tested with AG01522 primary normal human diploid fibroblasts. The surviving fraction of 15 μ M HA14-1-treated AG01522 cells was 50%,⁴¹⁾ showing that the cytotoxicity of HA14-1 in AG01522 cells was almost identical to that in Bcl-2 and Neo cells. However, in contrast to the case for Bcl-2 cells and Neo cells, pre-irradiation HA14-1 treatment did not affect the sensitivity of AG01522 cells to carbon ions and γ -rays,⁴¹⁾ predicting that HA14-1 may produce preferential radiosensitization of tumor cells.

Altogether, these findings highlight the notion that Bcl-2 might be an attractive target for improving the efficacy of heavy-ion therapy. The underlying mechanisms and the *in vivo* validity need to be further examined.

EFFECTS OF HEAVY IONS AND PHOTONS ON THE PROCESSES OF METASTASIS AND ANGIOGENESIS

Background

In recent years, radiotherapy has attained excellent local control and reduction of the damage to normal tissues as a result of the development of highly precise irradiation techniques such as stereotactic irradiation, intensity-modulated radiation therapy and particle radiotherapy. However, radiotherapy has been basically regarded as a local cancer therapy like surgery; one of the next concerns would hence be whether it is able to inhibit distant metastasis, the main cause of mortality in cancer patients. The metastatic process of malignant tumor cells generally consists of (i) detachment of cells from the primary tumor, (ii) migration to extracellular matrix (ECM), (iii) degradation of basement membrane, (iv) invasion into blood vessels, (v) circulation in blood flow, (vi) escape to extravascular matrices and (vii) implantation to target organs. Angiogenesis is not only a prerequisite for tumor growth and development, but is also a major factor affecting the metastatic spread of malignant cells. Here we discuss the effects of heavy-ion and photon irradiation on the processes of metastasis and angiogenesis.

Radiation effects on the process of metastasis

The first study of the effects of local X-ray irradiation on metastasis has been reported by Kaplan and Murphy in 1949,¹⁰⁸⁾ who showed that irradiated mice develop more frequent lung metastasis than untreated mice. Since then, a similar phenomenon has also been demonstrated by several investigators, but others have reported that the metastatic potential decreased after irradiation.¹⁰⁹⁾ Such discrepancy might be due to differences in tumor types, tumor ages, radiation doses and experimental design (especially the timing factor). According to a review by von Essen,¹⁰⁹⁾ four possible mechanisms that might influence the rate of metastasis following tumor irradiation can be considered: (i) direct alteration of tumor cells by irradiation, (ii) abscopal effect of local irradiation, (iii) local effect of irradiation facilitating entry of tumor cells into circulation and (iv) local effect of irradiation delaying tumor progression, thus allowing increased time for escape of tumor cells into circulation.

Recent progress in molecular biology has made it feasible to investigate the molecular mechanisms responsible for radiation effects on metastasis. Wild-Bode *et al.*¹¹⁰⁾ have reported that sublethal photon irradiation promotes the invasiveness of glioblastoma cells dose-dependently. The mechanism underlying this promotion of metastatic potential of cancer cells involved increased matrix metalloproteinase 2 (MMP-2) activity and upregulated expression of the cell-adhesion molecule integrin α V β 3. MMPs constitute a family of Zn²⁺-dependent enzymes essential for ECM turnover

under normal and pathological conditions.¹¹⁰⁾ Especially, MMP-2 can degrade type IV collagen, one of the major components of the basement membrane, resulting in the promotion of tumor invasion and metastasis.¹¹⁰⁾ There have been many reports on the enhancement of MMP-2 activity by photon irradiation.¹¹¹⁾ The integrin family of adhesion molecules is a class of ECM receptors consisting of multiple subtypes of α and β chains that, in combination, form various heterodimers with distinct cellular and adhesive characteristics.¹¹²⁾ Integrin-mediated adhesion to ECM triggers intracellular signaling that modulates cell proliferation, shape, migration, invasion and survival.¹¹³⁾ The vitronectin receptor, integrin α V β 3, also appears to be associated with increased invasiveness.¹¹⁴⁾ A monoclonal antibody against integrin α V β 3 abolishes such increased invasiveness, indicating that reduction of integrin α V β 3 can inhibit cell migration.¹¹⁵⁾ We have also confirmed that photon irradiation promotes cell migration capability concomitant with upregulation of integrin α V β 3 at a low dose.³⁴⁾

Qian *et al.*¹¹⁶⁾ reported that radiation increases the expression of hepatocyte growth factor (HGF) receptor/c-Met in pancreatic cancer cells *in vitro*. HGF is a stroma-derived cytokine that has multiple functions in various cell types including mitogenic, motogenic, morphogenic and antiapoptotic activities through a transmembrane tyrosine kinase receptor (c-Met). Radiation-enhanced expression of c-Met promotes HGF-mediated cell scattering and invasion.¹¹⁶⁾ A recombinant HGF antagonist can effectively inhibit photon-induced increases in invasive potential.¹¹⁶⁾ Overexpression of vascular endothelial growth factor (VEGF), an important growth factor in controlling angiogenesis, has been associated with tumor progression and metastasis. Photon irradiation enhanced the release/production of VEGF in human neuroblastoma cells, and these alterations have been associated with their increased metastatic potential.¹¹⁷⁾

In many solid tumors, the stroma is increasingly being recognized for its importance in promoting tumor proliferation, invasion and metastasis. Ohuchida *et al.*¹¹⁸⁾ demonstrated that photon-irradiated stromal fibroblasts strongly promote the invasiveness of pancreatic cancer cells through increased activation of HGF/c-Met signals compared with non-irradiated fibroblasts. An HGF antagonist blocks the increased invasiveness of pancreatic cancer cells when co-cultured with photon-irradiated fibroblasts.¹¹⁸⁾ Paquette *et al.*¹¹⁹⁾ found that irradiation of the basement membrane enhances the invasiveness of breast cancer cells with upregulation of MMP-2 and membrane type 1-MMP from cancer cells. Consequently, tumor-stroma interactions, which play a significant role in tumor development and metastasis, should provide important therapeutic targets.

High-LET carbon ions have been shown to be more effective for cell killing than photons. Only a few studies have addressed the effects of particle irradiation on the functioning of cells with metastatic potential. We hypothesized that

particle irradiation might inhibit the metastatic potential by ion beam-specific biological effects, and first focused on *in vitro* models including adhesion, migration, invasion, and the expression level and activity of molecules related to metastasis such as integrins α V β 3 and β 1, and MMP-2.³⁴⁾ Carbon-ion irradiation decreased cell migration and invasion in a dose-dependent manner and strongly inhibited MMP-2 activity.³⁴⁾ In carbon ion-irradiated cancer cells, the number of pulmonary metastases was decreased significantly *in vivo*.³⁴⁾ We further investigated the effect of carbon-ion irradiation on gene expression associated with metastasis and angiogenesis of non-small-cell lung cancer cells using microarray.¹²⁰⁾ Carbon-ion irradiation inhibited the gene expression of *ANLN* (anillin), which is involved in the activation of Rho and the phosphatidylinositol 3-kinase/Akt signaling pathway associated with cell migration.¹²⁰⁾ Goetze *et al.*¹²¹⁾ demonstrated that carbon-ion irradiation inhibited integrin expression, thus leading to the inhibition of migration ability *in vitro*.

Radiation effects on the process of angiogenesis

The process of tumor development requires adequate nutrition and oxygen. Usually, tumor mass cannot exceed a size limit of 1–2 mm diameter without blood vessel formation. Angiogenesis, the formation of new capillaries from pre-existing vessels, is a complex process of ECM degradation, migration and proliferation of endothelial cells and, finally, tube formation.¹²²⁾ Tumor vasculature is often structurally and functionally abnormal, and tortuous and leaky vasculature leads to interstitial hypertension, hypoxia and acidosis. Therefore, angiogenesis plays a key role in cancer cell survival, local tumor growth, and development of distant metastases. The combination of antiangiogenic agents and radiotherapy has been extensively investigated with the aim of improving therapeutic gain in preclinical and clinical settings.

Some studies have shown that low-dose irradiation of endothelial cells induces angiogenic factors, promoting angiogenesis. Sonveaux *et al.*¹²³⁾ reported that low-dose photons activate the nitric oxide pathway in endothelial cells, leading to phenotypic changes promoting tumor angiogenesis. A nitric oxide synthase inhibitor prevents photon-induced tube formation.¹²³⁾ Abdollahi *et al.*¹²⁴⁾ found that photons increase VEGF and basic fibroblast growth factor in prostate cancer cells and VEGF receptor in endothelial cells. In a co-culture invasion model of prostate cancer cells and endothelial cells, selective irradiation of cancer cells promotes endothelial cell invasion through the basement membrane.¹²⁴⁾ Receptor tyrosine kinase inhibitors attenuate endothelial cell invasion in response to irradiated cancer cells in the co-culture model.¹²⁴⁾

The inhibition of further tumor growth by tumor mass is generally observed in some clinical and experimental malignancies due to the production of angiogenesis inhibitors by

the primary tumor. Therefore, removal of the primary tumor can be followed by the rapid growth of distant subclinical metastases.¹²⁵ These phenomena are similar to that reported by Camphausen *et al.*¹²⁶ in the eradication of photon-treated primary tumor. Administration of recombinant angiostatin, an angiogenesis inhibitor, suppresses the growth of the metastases after local control of the primary tumor with radiotherapy.¹²⁶ This means that combination treatment with angiogenesis inhibitor offers the promise of control of distant metastasis, thus improving the therapeutic gain.

It is well known that hypoxia contributes to radioresistance, i.e., a lack of oxygen to facilitate DNA damage. Therefore, there is concern that a reduction in tumor oxygenation resulting from inhibition of angiogenesis with destruction of the tumor vasculature could render the tumor hypoxic and thereby more radioresistant. Wachsberger *et al.*¹²⁷ observed that treatment with a tumor vasculature-damaging agent when given at an inappropriate time prior to irradiation results in less antitumor activity compared with radiotherapy alone. This result can be explained by tumor hypoxia induced by the agent. However, most researchers have shown that antiangiogenic agents can enhance the tumor response to radiation.¹²⁸ Jain¹²⁹ has proposed that the angiogenesis inhibitor can also transiently normalize the abnormal structure and function of tumor vasculature to make it more efficient for oxygen and drug delivery. Additional work is awaited to determine the optimal timing and duration of antiangiogenic therapy combined with radiotherapy for maximizing therapeutic gain.

Little is known about the effects of heavy ions on cell function associated with angiogenesis. We hypothesized that particle irradiation might inhibit angiogenesis as well as the metastatic potential of cancer cells. To confirm this hypothesis, we used *in vitro* models to observe the expression level and activity of molecules related to metastasis such as integrin α V β 3 and MMP-2.³³ After carbon-ion irradiation, the adhesiveness and migration of cancer cells to vitronectin were inhibited and the capillary-like tube structures formed by cancer cells in three-dimensional culture were destroyed, concomitant with the inhibition of MMP-2 activity and downregulation of integrin α V β 3.³³ Surprisingly, these structures could be destroyed even at a dose as low as 0.1 Gy.³³ Therefore, these results suggest that destruction of the vascular structure may not be induced by inhibition of endothelial cell growth but by other mechanisms such as inhibition of MMP-2 and downregulation of integrin α V β 3.

Conclusion

Many investigators have shown that photon irradiation enhances the metastatic process of malignant tumor cells and angiogenesis at a sublethal dose. Although the molecular mechanisms underlying these phenomena seem complex, tumor-stroma interactions may play a significant role in tumor development and metastasis. Heavy-ion irradiation

suppresses the metastatic potential of cancer cells and angiogenesis even at lower doses. Particle radiotherapy may be superior to conventional photon therapy in its possible effects for the prevention of metastasis of irradiated malignant tumor cells in addition to its physical dose distribution. Further intensive studies are also necessary to elucidate the relevant molecular mechanisms involved in angiogenesis- and invasion-related molecules specifically associated with particle irradiation.

BREAST CANCER INDUCTION BY LOW-DOSE HEAVY-ION RADIATION

Background of heavy ion-induced carcinogenesis

Based on many biological advantages as discussed in previous sections, continuing efforts to improve heavy-ion therapy have established more accurate control of cancer and longer patient survival than conventional photon therapy and, hence, its utilization has steadily spread. In turn, however, the potential risk for late adverse effects, especially for developing secondary cancers, is becoming a new matter of concern. Knowledge is therefore required concerning the secondary cancer risk from heavy-ion radiation; nevertheless, such information is still very scarce in both epidemiological and experimental aspects.

Breast (mammary gland) is one of the organs irradiated during radiotherapy for the chest area and is a susceptible organ to the cancer-inducing effect of low-LET radiation. Its high susceptibility to cancer after irradiation has been revealed by epidemiological studies on Japanese atomic bomb survivors and medically irradiated subjects.^{130,131} Compared to the background breast cancer incidence, the risk of female breast cancer after low-LET irradiation increases as a linear function of dose by 0.87-fold per Gy (i.e., the excess relative risk is 0.87/Gy).¹³⁰ In contrast, there is no such information on human breast cancer risk from heavy ions. Nevertheless, it is of note that neutron radiation is reported to have a very high RBE of 13 to 100 at lower doses^{132,133} for induction of rat mammary cancer, a widely used animal model of human breast cancer.¹³⁴ The very high RBE of neutrons renders it an important subject to clarify whether the RBE of heavy ions is similarly high. However, there are only limited data available on mammary gland carcinogenesis by heavy ions from the BEVALAC synchrotron at the University of California, Berkeley, USA, the AGS synchrotron at the Brookhaven National Laboratory, USA, and the HIMAC synchrotron (Table 2).¹³⁵⁻¹³⁷

The SOBP carbon-ion beam (LET, 40–90 keV/ μ m) from HIMAC has been intensively used to treat cancers of various sites since 1994.⁷ Several animal experiments have been conducted to determine the effect of carbon ions from HIMAC on the induction of tumors of the skin, kidney, stomach, adrenal, ovary and thymus,¹³⁸⁻¹⁴² and recent reviews have elegantly covered such information on carcino-

Table 2. Relative biological effectiveness (RBE) of high linear energy transfer radiation for induction of rat mammary cancer.

Particle	Energy	Strain	Dose (Gy)	RBE	Dose response curve
Neutron ¹³²⁾	430 keV	Sprague-Dawley	0.001–0.06	13–100	Convex upward
Neutron ¹³³⁾	0.5 MeV	WAG/Rij	0.05–0.2	9–14	Linear
Neon ion ¹³⁵⁾	6.6 GeV	Sprague-Dawley	0.02	> 5	Linear
Iron ion ¹³⁶⁾	1 GeV	Sprague-Dawley	0.05–0.16	< 10 *	Linear
Carbon ion ¹³⁷⁾	290 MeV	Sprague-Dawley	0.05–1	2–10	Convex upward

* The end point of the experiment was the development of overall mammary tumors including both cancer and benign tumors.

genesis in experimental animal models.^{2,143)} In this section, we briefly summarize some features of experimental carcinogenesis by heavy ions, focusing on the rat mammary cancer model.

Dose-effect relationship and RBE

Shellabarger and colleagues¹³⁵⁾ have investigated the induction of Sprague-Dawley rat mammary cancer after exposure to neon ions (0.02–0.54 Gy; LET, 33 keV/ μ m) from BEVALAC and to X-rays (0.57–1.71 Gy). The dose response for neon ions was linear up to 0.54 Gy, and the RBE was roughly estimated to be > 5 at the incidence of 20% (i.e., ~0.02 Gy of neon ions; Fig. 7a).¹³⁵⁾ Imaoka *et al.*¹³⁷⁾ also used the Sprague-Dawley rat to compare the carcinogenic effects of carbon ions (0.05–2 Gy; LET, 40–90 keV/ μ m) from HIMAC and γ -rays (0.5–2 Gy). Therein, the dose response for carbon ions was convex upward and well-fitted by a square-root function of dose (Fig. 7b).¹³⁷⁾ As the dose response for γ -rays was linear, these fittings resulted in a dose-dependent RBE, which yielded 10 and 2 at 0.05 and 1 Gy, respectively.¹³⁷⁾ In addition, an interim result has reported an RBE of < 10 for iron ions from AGS (0.05–2 Gy; LET, 155 keV/ μ m), although this analysis did not separate benign tumors and cancers.¹³⁶⁾ Those three studies obtained similar RBE, suggesting that high-LET heavy ions (33 and 40–90 keV/ μ m) have high RBE for rat mammary cancer induction comparable to the reported high values of neutrons (Table 2).

Modulation by genetic factors

Genetic background is an important factor influencing cancer susceptibility, and in this respect rat strains with different genetic backgrounds have provided a good animal model.¹³⁴⁾ For example, comparison of the susceptibility to chemically-induced mammary carcinogenesis among a series of rat strains has showed that the Sprague-Dawley, WF and Lewis strains have the highest susceptibility, whereas F344 and ACI strains have moderate-to-low susceptibility (Fig. 8a).¹⁴⁴⁾ Regarding X-ray-induced mammary carcino-

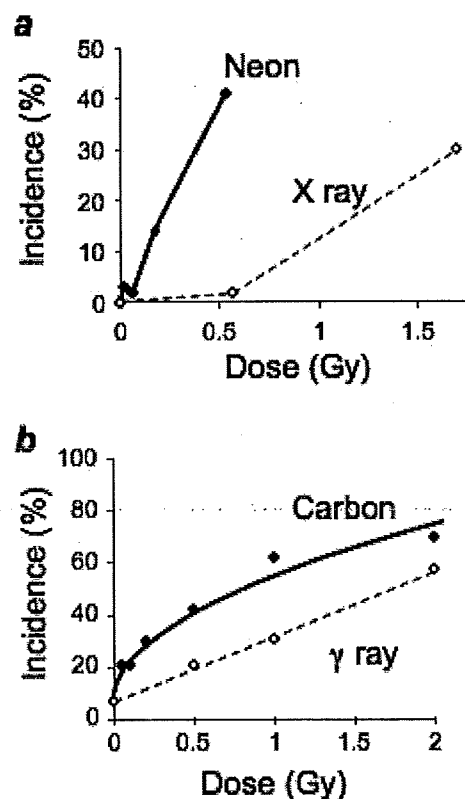


Fig. 7. Dose effect relationship of heavy ion- and low linear energy transfer radiation-induced rat mammary carcinogenesis. Shown is the incidence of mammary cancer after exposure to 6.6 GeV/u neon ions (closed circles) and X-rays (open circles) (Panel a) and 290 MeV/u carbon ions (closed circles) and γ -rays (open circles) (Panel b). Constructed from data presented in Shellabarger *et al.*¹³⁵⁾ (a) and Imaoka *et al.*¹³⁷⁾ (b).

genesis, comparison of published data implies that susceptibility is high in Sprague-Dawley,^{135,145,146)} moderate in Lewis¹⁴⁶⁾ and low in ACI¹⁴⁷⁾ and F344¹⁴⁸⁾ strains (Fig. 8b). Of note, X-rays show strong carcinogenicity when combined with estrogen treatment in ACI rats.¹⁴⁷⁾ In the neutron induc-

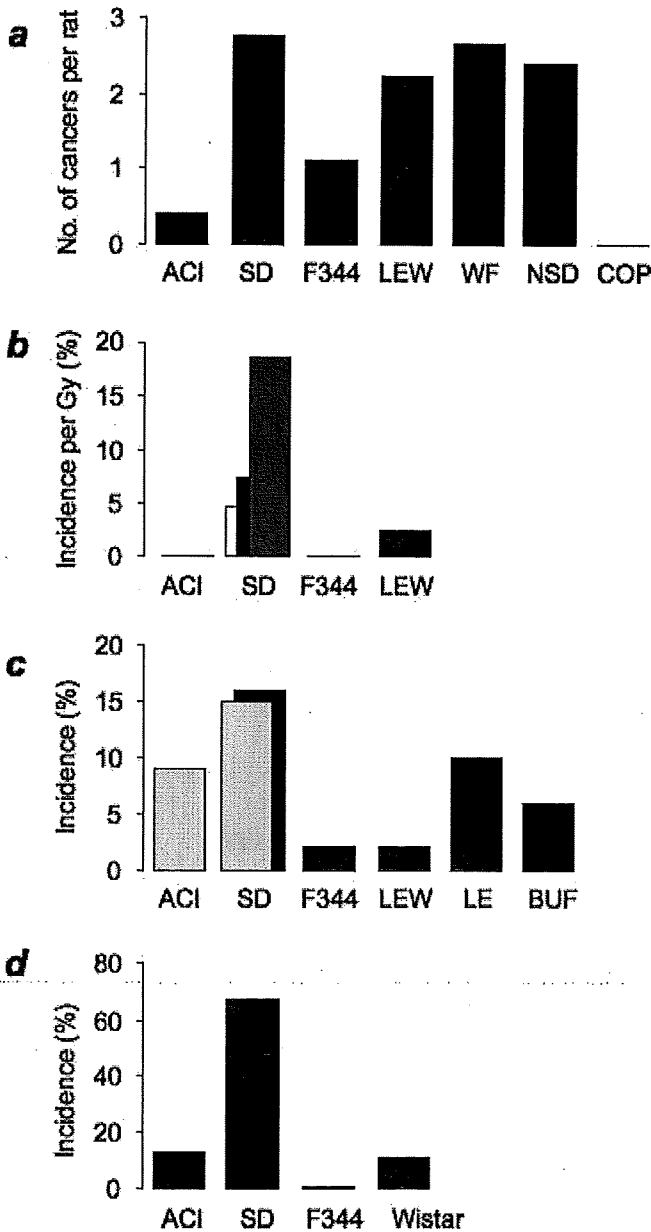


Fig. 8. Rat strain difference in susceptibility to mammary carcinogens. Panel *a*, The average number of cancers per rat after exposure to the chemical carcinogen 7,12-dimethylbenz(a)anthracene.¹⁴⁴ Panel *b*, Slope of linear equations fitted to dose-effect relationship for X-ray-induced mammary cancer incidence. Sprague-Dawley (data from three literatures are shown by white,¹⁴⁵ black¹⁴⁶ and gray¹³⁵ columns), F344¹⁴⁸ and Lewis¹⁴⁶ rats were observed for 300–350 days, and ACI rats for 190 days.¹⁴⁷ Panel *c*, Incidence of mammary cancer after exposure to 0.05 Gy of fission neutrons¹⁵⁰ (black column) and 0.004 Gy of 430 keV fast neutrons¹⁴⁹ (gray column). Panel *d*, Incidence of mammary cancer after exposure to 1 Gy of 290 MeV/u carbon ions with a spread-out Bragg peak.¹³⁷ All graphs were constructed from data in indicated literature. SD, Sprague-Dawley; LEW, Lewis; WF, Wistar-Furth; LE, Long-Evans; BUF, Buffalo.

tion models, the Sprague-Dawley strain has been identified as being highly susceptible in contrast to F344 and Lewis strains (Fig. 8c).^{149,150} In addition, the Sprague-Dawley rat also has higher susceptibility to heavy ion-induced carcinogenesis than F344 and ACI strains (Fig. 8d).¹³⁷ The high susceptibility of the Sprague-Dawley strain thus seems to be independent of the carcinogen species. Given that variations in cancer susceptibility also exist for human populations, secondary cancer risk after heavy-ion therapy might well differ among individuals.

Biological characteristics of induced tumors

Although the biological characteristics of heavy ion-induced cancers are poorly understood, some insights are available from animal experiments. Data on neon ion-irradiated rats have indicated that the incidence of fibroadenoma (a benign tumor) of the mammary gland was higher than that of carcinoma (or cancer).¹³⁵ The same tendency has been observed in carbon ion-, X-ray- and γ -ray-irradiated rats.^{135,137} Iron ion-induced mammary cancers have also been reported to contain fibroadenoma and carcinoma.¹³⁶ Such high prevalence of fibroadenoma is characteristic of radiation induction models, making a stark contrast to chemical induction, where carcinoma predominantly develops.¹⁴⁴ In addition, carbon ion-induced mammary cancer is reported to be highly metastatic to lung compared to γ -ray-induced one.¹³⁷ As metastasis has been observed after irradiation with a dose as low as 0.05 Gy,¹³⁷ it is unlikely that heavy ion-induced tissue reactions of the lung have promoted the metastatic process. The mechanism underlying the strong metastatic potential is currently unclear.

The ovarian hormone estrogen plays important roles in the development of most mammary cancers, and estrogen receptor expression is indicative of the hormone dependence of tumors. Because the majority (> 70%) of both carbon ion- and γ -ray-induced mammary cancers express estrogen receptor,¹³⁷ estrogen may play crucial roles in both models. The *H-ras* protooncogene is an estrogen-regulated gene, and its mutation, together with its induction by estrogen, plays a major role in chemically-induced rat mammary carcinogenesis.¹⁵¹ Carbon ion-induced rat mammary cancer is, however, devoid of *H-ras* mutations, as is γ -ray-induced cancer, nor does it have *p53* mutation.¹³⁷ Thus, causative gene mutation for heavy-ion induction remains unidentified. Because comprehensive genetic analysis using microarray has revealed altered genes in γ -ray-induced rat mammary cancer,¹⁵² such analysis on heavy ion-induced cancers is indeed warranted.

Implication for secondary cancer risk from medical exposure

Evidence suggests that heavy ions with LET of 33 and 40–90 keV/ μ m have high RBE for inducing mammary cancer in the Sprague-Dawley rat. Normal tissue in the close

vicinity of cancer may be exposed to the high-LET component of the SOBP beam during therapy and thus be at high risk of developing secondary cancer. In contrast, low-LET carbon ions (~13 keV/ μm) have both low *in vitro* transformation efficiency¹⁵³⁾ and weak tumorigenicity *in vivo*,¹³⁹⁾ suggesting a relatively low risk from exposure of normal tissue to therapeutic heavy-ion beams. The variable sensitivity among rat strains implies that individual cancer susceptibility need to be taken into account, such as genetic polymorphisms related to breast cancer risk (e.g., *BRCA* genes). More information from experimental carcinogenesis study is awaited for a more concrete estimation of secondary cancer risk from heavy-ion therapy.

PERSPECTIVES

In spite of a series of studies, how heavy ions inactivate cells more effectively than photons continues to remain a fascinating question. The question concerning the LET dependence of induction of DNA DSBs and clustered DNA damage is still fully open.^{11,12)} Growing evidence now suggests that heavy ions kill cells via various modes of cell death (e.g., autophagy and premature senescence in addition to apoptosis) and overcome radioresistance, although the current evidence is still only phenomenological. A deeper understanding of the mechanism of action of heavy ions and the molecular underpinnings of heavy ion-induced cell death would be necessary, which may in turn lead to (i) mechanism-based designing of biological approaches that enhance tumor control without aggravating, or even with assuaging, normal tissue complications, (ii) prediction of both the heavy-ion responsiveness of tumors and normal tissue complications (including acute reactions and secondary cancers) prior to treatment and (iii) tailor-made therapy for individual patients. In this regard, recent studies have been conducted to molecularly profile the heavy-ion response of tumor cells irradiated *in vivo*,^{154,155)} and this encourages further investigation to clarify the genes responsible for susceptibility to heavy ions.

ACKNOWLEDGMENTS

N. H. and Y. K. are indebted to Drs. Takamitsu Hara, Sakura Hamada, Keiko Kataoka (Gunma Univ., Japan), Tetsuya Sakashita, Tomoo Funayama and Yuichiro Yokota (JAEA, Japan) for help with irradiation experiments; the work was supported in part by a Grant-in-Aid for the 21st Century Center-of-Excellence Program for Biomedical Research Using Accelerator Technology to Gunma University Graduate School of Medicine from the Ministry of Education, Culture Sports, Science and Technology (MEXT) of Japan, and by the budget of Nuclear Research of MEXT based on screening and counseling by the Atomic Energy Commission of Japan. T. I. and Y. S. acknowledge Drs.

Mayumi Nishimura, Shizuko Kakinuma, Takashi Takabatake, Kazuhiko Daino (NIRS, Japan) and Daisuke Iizuka (Hiroshima Univ., Japan) for kind collaboration and critical reading of the manuscript; the work was supported in part by a research grant from the Takeda Science Foundation, and Grants-in-Aid for Young Scientists (B) (No. 20710049) from MEXT and for Scientific Research (A and C) (No. 19201011 and 21610029) from the Japan Society for the Promotion of Science (JSPS), and Health and Labor Sciences Research Grants (No. 19141201 and 19S-1) from the Ministry of Health, Labor and Welfare of Japan. S. M. and K. O. acknowledge Drs. Ryoichi Hirayama and Akiko Uzawa (NIRS, Japan) for dedicated support for animal experiments; the work was supported in part by Grants-in-Aid for Scientific Research (C) (No. 18591380 and 20591493) from JSPS. T. Ogata and T. T. acknowledge Drs. Nariaki Matsuura, Yutaka Takahashi (Osaka Univ., Japan) and Yoshiya Furusawa (NIRS, Japan). R. O. and T. K. greatly appreciate Drs. Akira Fujimori, Miho Noguchi, Mr. Kentaro Seo and Mr. Yoshihiro Fujii (NIRS, Japan) for invaluable help in preparing the manuscript; the work was supported by a Grant-in-Aid for Scientific Research (A) (No. 16209036) from JSPS. A. T. and T. Ohnishi acknowledge Drs. Tadaaki Kirita and Nobuhiro Yamakawa (Nara Medical Univ., Japan); the work was supported by Grants-in-Aid for Scientific Research from MEXT, a grant from the Central Research Institute of Electric Power Industry, and a grant for Exploratory Research for Space Utilization from the Japan Space Forum. Some works herein were conducted as part of the Research Project with Heavy Ions at NIRS-HIMAC. The cost for the English editing of the manuscript was supported by Space Radiation Research Unit, International Open Laboratory, NIRS, Japan, and the authors are grateful to Dr. Yukio Uchihori (NIRS, Japan).

REFERENCES

1. Fokas E, *et al* (2009) Ion beam radiobiology and cancer: Time to update ourselves. *Biochim Biophys Acta* **1796**: 216–229.
2. Ando K and Kase Y (2009) Biological characteristics of carbon-ion therapy. *Int J Radiat Biol* **85**: 715–728.
3. Blakely EA and Chang PY (2009) Biology of charged particles. *Cancer J* **15**: 271–284.
4. Hamada N (2009) Recent insights into the biological action of heavy-ion radiation. *J Radiat Res* **50**: 1–9.
5. Kanai T, *et al* (1997) Irradiation of mixed beam and design of spread-out Bragg peak for heavy-ion radiotherapy. *Radiat Res* **147**: 78–85.
6. Castro JR, *et al* (1994) Experience in charged particle irradiation of tumors of the skull base: 1977–1992. *Int J Radiat Oncol Biol Phys* **29**: 647–655.
7. Tsujii H, *et al* (2007) Clinical results of carbon ion radiotherapy at NIRS. *J Radiat Res* **48**: A1–A13.
8. Schulz-Ertner D and Tsujii H (2007) Particle radiation therapy using proton and heavier ion beams. *J Clin Oncol* **25**: 953–964.

9. Durante M, *et al* (2000) X-rays vs. carbon-ion tumor therapy: cytogenetic damage in lymphocytes. *Int J Radiat Oncol Biol Phys* **47**: 793–798.
10. Hall EJ and Giaccia AJ (2006) *Radiobiology for the Radiologist*. 6 ed. Lippincott Williams & Wilkins, Philadelphia.
11. Terato H, *et al* (2008) Quantitative analysis of isolated and clustered DNA damage induced by γ -rays, carbon ion beams, and iron ion beams. *J Radiat Res* **49**: 133–146.
12. Hada M and Georgakilas AG (2008) Formation of clustered DNA damage after high-LET irradiation: a review. *J Radiat Res* **49**: 203–210.
13. Tsuruoka C, *et al* (2008) The difference in LET and ion species dependence for induction of initially measured and non-rejoined chromatin breaks in normal human fibroblasts. *Radiat Res* **170**: 163–171.
14. Suzuki M, *et al* (2006) Cellular and molecular effects for mutation induction in normal human cells irradiated with accelerated neon ions. *Mutat Res* **594**: 86–92.
15. Tsuruoka C, *et al* (2005) LET and ion species dependence for cell killing in normal human skin fibroblasts. *Radiat Res* **163**: 494–500.
16. Hino M, *et al* (2009) Insufficient membrane fusion in dysferlin-deficient muscle fibers after heavy-ion irradiation. *Cell Struct Funct* **34**: 11–15.
17. Hino M, *et al* (2007) Heavy ion microbeam irradiation induces ultrastructural changes in isolated single fibers of skeletal muscle. *Cell Struct Funct* **32**: 51–56.
18. Oishi T, *et al* (2008) Proliferation and cell death of human glioblastoma cells after carbon-ion beam exposure: morphologic and morphometric analyses. *Neuropathology* **28**: 408–416.
19. Jinno-Oue A, *et al* (2010) Irradiation with carbon ion beams induces apoptosis, autophagy, and cellular senescence in a human glioma-derived cell line. *Int J Radiat Oncol Biol Phys* **76**: 229–241.
20. Al-Jahdari WS, *et al* (2009) The radiobiological effectiveness of carbon-ion beams on growing neurons. *Int J Radiat Biol* **85**: 700–709.
21. Kawamura H, *et al* (2009) Ceramide induces myogenic differentiation and apoptosis in *Drosophila* Schneider cells. *J Radiat Res* **50**: 161–169.
22. Harada K, *et al* (2009) Heavy-ion-induced bystander killing of human lung cancer cells: role of gap junctional intercellular communication. *Cancer Sci* **100**: 684–688.
23. Hamada N, *et al* (2008) Temporally distinct response of irradiated normal human fibroblasts and their bystander cells to energetic heavy ions. *Mutat Res* **639**: 35–44.
24. Hamada N, *et al* (2008) Energetic heavy ions accelerate differentiation in the descendants of irradiated normal human diploid fibroblasts. *Mutat Res* **637**: 190–196.
25. Wang J, *et al* (2008) The influence of fractionation on cell survival and premature differentiation after carbon ion irradiation. *J Radiat Res* **49**: 391–398.
26. Hamada N, *et al* (2008) The survival of heavy ion-irradiated Bcl-2 overexpressing radioresistant tumor cells and their progeny. *Cancer Lett* **268**: 76–81.
27. Kanasugi Y, *et al* (2007) Role of DNA-PKcs in the bystander effect after low- or high-LET irradiation. *Int J Radiat Biol* **83**: 73–80.
28. Hamada N, *et al* (2007) Intercellular and intracellular signaling pathways mediating ionizing radiation-induced bystander effects. *J Radiat Res* **48**: 87–95.
29. Hamada N, *et al* (2006) LET-dependent survival of irradiated normal human fibroblasts and their descendants. *Radiat Res* **166**: 24–30.
30. Hamada N (2009) The bystander response to heavy-ion radiation: intercellular signaling between irradiated and non-irradiated cells. *Biol Sci Space* **23**: in press.
31. Kakizaki T, *et al* (2006) Killing of feline T-lymphocytes by γ -rays and energetic carbon ions. *J Vet Med Sci* **68**: 1269–1273.
32. Kakizaki T, *et al* (2007) Vulnerability of feline T-lymphocytes to charged particles. *J Vet Med Sci* **69**: 605–609.
33. Takahashi Y, *et al* (2003) Heavy ion irradiation inhibits *in vitro* angiogenesis even at sublethal dose. *Cancer Res* **63**: 4253–4257.
34. Ogata T, *et al* (2005) Particle irradiation suppresses metastatic potential of cancer cells. *Cancer Res* **65**: 113–120.
35. Amino M, *et al* (2006) Heavy ion radiation up-regulates Cx43 and ameliorates arrhythmogenic substrates in hearts after myocardial infarction. *Cardiovasc Res* **72**: 412–421.
36. Mori E, *et al* (2009) High LET heavy ion radiation induces p53-independent apoptosis. *J Radiat Res* **50**: 37–42.
37. Hamada N, *et al* (2008) Energetic heavy ions overcome tumor radioresistance caused by overexpression of *Bcl-2*. *Radiother Oncol* **89**: 231–236.
38. Masunaga S, *et al* (2008) Radiobiologic significance of response of intratumor quiescent cells *in vivo* to accelerated carbon ion beams compared with γ -rays and reactor neutron beams. *Int J Radiat Oncol Biol Phys* **70**: 221–228.
39. Masunaga S and Ono K (2002) Significance of the response of quiescent cell populations within solid tumors in cancer therapy. *J Radiat Res* **43**: 11–25.
40. Nakano T, *et al* (2006) Carbon-beam therapy overcomes the radiation resistance of uterine cervical cancer originating from hypoxia. *Clin Cancer Res* **12**: 2185–2190.
41. Hamada N, *et al* (2008) The small-molecule Bcl-2 inhibitor HA14-1 sensitizes cervical cancer cells, but not normal fibroblasts, to heavy-ion radiation. *Radiother Oncol* **89**: 227–230.
42. Kitabayashi H, *et al* (2006) Synergistic growth suppression induced in esophageal squamous cell carcinoma cells by combined treatment with docetaxel and heavy carbon-ion beam irradiation. *Oncol Rep* **15**: 913–918.
43. Linstadt D, *et al* (1988) Radiosensitization produced by iododeoxyuridine with high linear energy transfer heavy ion beams. *Int J Radiat Oncol Biol Phys* **15**: 703–710.
44. Takahashi A, *et al* (2000) The dependence of p53 on the radiation enhancement of thermosensitivity at different LET. *Int J Radiat Oncol Biol Phys* **47**: 489–494.
45. Takahashi A, *et al* (2001) p53-dependent thermal enhancement of cellular sensitivity in human squamous cell carcinomas in relation to LET. *Int J Radiat Biol* **77**: 1043–1051.
46. Takahashi A, *et al* (2003) p53-dependent hyperthermic enhancement of tumour growth inhibition by X-ray or carbon-ion beam irradiation. *Int J Hyperthermia* **19**: 145–153.
47. Oohira G, *et al* (2004) Growth suppression of esophageal squamous cell carcinoma induced by heavy carbon-ion

- beams combined with *p53* gene transfer. *Int J Oncol* **25**: 563–569.
48. Duan X, *et al* (2008) Apoptosis of murine melanoma cells induced by heavy-ion radiation combined with *Tp53* gene transfer. *Int J Radiat Biol* **84**: 211–217.
 49. Monobe M and Ando K (2002) Drinking beer reduces radiation-induced chromosome aberrations in human lymphocytes. *J Radiat Res* **43**: 237–245.
 50. Monobe M, Arimoto-Kobayashi S and Ando K (2003) β -Pseudouridine, a beer component, reduces radiation-induced chromosome aberrations in human lymphocytes. *Mutat Res* **538**: 93–99.
 51. Monobe M, *et al* (2003) Effects of beer administration in mice on acute toxicities induced by X rays and carbon ions. *J Radiat Res* **44**: 75–80.
 52. Monobe M, *et al* (2005) Glycine betaine, a beer component, protects radiation-induced injury. *J Radiat Res* **46**: 117–121.
 53. Monobe M, *et al* (2006) Effects of glycine betaine on bone marrow death and intestinal damage by γ rays and carbon ions. *Radiat Prot Dosimetry* **122**: 494–497.
 54. Zhou G, *et al* (2006) Protective effects of melatonin against low- and high-LET irradiation. *J Radiat Res* **47**: 175–181.
 55. Shirazi A, Ghobadi G and Ghazi-Khansari M (2007) A radiobiological review on melatonin: a novel radioprotector. *J Radiat Res* **48**: 263–272.
 56. Manda K, Ueno M and Anzai K (2008) Melatonin mitigates oxidative damage and apoptosis in mouse cerebellum induced by high-LET ^{56}Fe particle irradiation. *J Pineal Res* **44**: 189–196.
 57. Manda K, Ueno M and Anzai K (2008) Memory impairment, oxidative damage and apoptosis induced by space radiation: ameliorative potential of α -lipoic acid. *Behav Brain Res* **187**: 387–395.
 58. Alpen EL, *et al* (1993) Tumorigenic potential of high-Z, high-LET charged-particle radiations. *Radiat Res* **136**: 382–391.
 59. Fry RJ, *et al* (1985) High-LET radiation carcinogenesis. *Radiat Res Suppl* **8**: S188–S195.
 60. Okada T, *et al* (2010) Carbon ion radiotherapy: clinical experiences at NIRS. *J Radiat Res* **51**: 00–00.
 61. Minohara S, *et al* (2010) Recent innovations in carbon ion radiotherapy. *J Radiat Res* **51**: 00–00.
 62. Rydberg B, Lobrich M and Cooper PK (1994) DNA double-strand breaks induced by high-energy neon and iron ions in human fibroblasts. I. Pulsed-field gel electrophoresis method. *Radiat Res* **139**: 133–141.
 63. Taucher-Scholz G, Heilmann J and Kraft G (1996) Induction and rejoining of DNA double-strand breaks in CHO cells after heavy ion irradiation. *Adv Space Res* **18**: 83–92.
 64. Iliakis G, Mehta R and Jackson M (1992) Level of DNA double-strand break rejoining in Chinese hamster xrs-5 cells is dose-dependent: implications for the mechanism of radiosensitivity. *Int J Radiat Biol* **61**: 315–321.
 65. Noguchi M, *et al* (2006) Inhibition of homologous recombination repair in irradiated tumor cells pretreated with Hsp90 inhibitor 17-allylamino-17-demethoxygeldanamycin. *Biochem Biophys Res Commun* **351**: 658–663.
 66. Rothkamm K and Lobrich M (2003) Evidence for a lack of DNA double-strand break repair in human cells exposed to very low x-ray doses. *Proc Natl Acad Sci USA* **100**: 5057–5062.
 67. Kato TA, *et al* (2006) γH2AX foci after low-dose-rate irradiation reveal atm haploinsufficiency in mice. *Radiat Res* **166**: 47–54.
 68. Cornforth MN and Bedford JS (1983) X-ray-induced breakage and rejoining of human interphase chromosomes. *Science* **222**: 1141–1143.
 69. Okayasu R, Cheong N and Iliakis G (1993) Technical note: comparison of yields and repair kinetics of interphase chromosome breaks visualized by Sendai-virus or PEG-mediated cell fusion in irradiated CHO cells. *Int J Radiat Biol* **64**: 689–694.
 70. Sekine E, *et al* (2008) High LET heavy ion radiation induces lower numbers of initial chromosome breaks with minimal repair than low LET radiation in normal human cells. *Mutat Res* **652**: 95–101.
 71. Iliakis GE and Pantelias GE (1990) Production and repair of chromosome damage in an X-ray sensitive CHO mutant visualized and analysed in interphase using the technique of premature chromosome condensation. *Int J Radiat Biol* **57**: 1213–1223.
 72. Fukumura R, *et al* (2003) A sensitive transcriptome analysis method that can detect unknown transcripts. *Nucleic Acids Res* **31**: e94.
 73. Fujimori A, *et al* (2005) Extremely low dose ionizing radiation up-regulates CXC chemokines in normal human fibroblasts. *Cancer Res* **65**: 10159–10163.
 74. Fujimori A, *et al* (2008) Ionizing radiation downregulates *ASPM*, a gene responsible for microcephaly in humans. *Biochem Biophys Res Commun* **369**: 953–957.
 75. Bird RP and Burki HJ (1975) Survival of synchronized Chinese hamster cells exposed to radiation of different linear-energy transfer. *Int J Radiat Biol* **27**: 105–120.
 76. Wang H, *et al* (2009) S-phase cells are more sensitive to high-linear energy transfer radiation. *Int J Radiat Oncol Biol Phys* **74**: 1236–1241.
 77. Vaupel P (2004) Tumor microenvironmental physiology and its implications for radiation oncology. *Semin Radiat Oncol* **14**: 198–206.
 78. Jain RK (1989) Delivery of novel therapeutic agents in tumors: physiological barriers and strategies. *J Natl Cancer Inst* **81**: 570–576.
 79. Masunaga S, *et al* (1990) Use of the micronucleus assay for the selective detection of radiosensitivity in BUdR-unincorporated cells after pulse-labelling of exponentially growing tumour cells. *Int J Radiat Biol* **58**: 303–311.
 80. Masunaga S, Ono K and Abe M (1991) A method for the selective measurement of the radiosensitivity of quiescent cells in solid tumors-combination of immunofluorescence staining to BrdU and micronucleus assay. *Radiat Res* **125**: 243–247.
 81. Masunaga S, *et al* (1994) The radiosensitivity of quiescent cell populations in murine solid tumors in irradiation with fast neutrons. *Int J Radiat Oncol Biol Phys* **29**: 239–242.
 82. Masunaga S, *et al* (1998) Response of quiescent and total tumor cells in solid tumors to neutrons with various cadmium ratios. *Int J Radiat Oncol Biol Phys* **41**: 1163–1170.
 83. Masunaga S, *et al* (1999) Repair of potentially lethal damage

- by total and quiescent cells in solid tumors following a neutron capture reaction. *J Cancer Res Clin Oncol* **125**: 609–614.
84. Masunaga S, *et al* (1999) Reoxygenation in quiescent and total intratumor cells following thermal neutron irradiation with or without ^{10}B -compound-compared with that after γ -ray irradiation. *Int J Radiat Oncol Biol Phys* **44**: 391–398.
 85. Torikoshi M, *et al* (2007) Irradiation system for HIMAC. *J Radiat Res* **48**: A15–A25.
 86. Masunaga S, *et al* (2009) The effect of post-irradiation tumor oxygenation status on recovery from radiation-induced damage *in vivo*: with reference to that in quiescent cell populations. *J Cancer Res Clin Oncol* **135**: 1109–1116.
 87. Hollstein M, *et al* (1991) *p53* mutations in human cancers. *Science* **253**: 49–53.
 88. Takahashi A (2001) Different inducibility of radiation- or heat-induced *p53*-dependent apoptosis after acute or chronic irradiation in human cultured squamous cell carcinoma cells. *Int J Radiat Biol* **77**: 215–224.
 89. Asakawa I, *et al* (2002) Radiation-induced growth inhibition in transplanted human tongue carcinomas with different *p53* gene status. *Anticancer Res* **22**: 2037–2043.
 90. Kirita T, Ohnishi K and Ohnishi T (2001) A new strategy for cancer therapy based on a predictive indicator. *Hum Cell* **14**: 1–6.
 91. Lane DP (1992) Cancer. *p53*, guardian of the genome. *Nature* **358**: 15–16.
 92. Takahashi A, *et al* (2008) DNA damage recognition proteins localize along heavy ion induced tracks in the cell nucleus. *J Radiat Res* **49**: 645–652.
 93. Takahashi A, *et al* (2005) Apoptosis induced by high-LET radiations is not affected by cellular *p53* gene status. *Int J Radiat Biol* **81**: 581–586.
 94. Takahashi A, *et al* (2004) High-LET radiation enhanced apoptosis but not necrosis regardless of *p53* status. *Int J Radiat Oncol Biol Phys* **60**: 591–597.
 95. Aoki M, Furusawa Y and Yamada T (2000) LET dependency of heavy-ion induced apoptosis in V79 cells. *J Radiat Res* **41**: 163–175.
 96. Coelho D, *et al* (2002) Induction of apoptosis by high linear energy transfer radiation: role of *p53*. *Can J Physiol Pharmacol* **80**: 644–649.
 97. Yamakawa N, *et al* (2008) High LET radiation enhances apoptosis in mutated *p53* cancer cells through Caspase-9 activation. *Cancer Sci* **99**: 1455–1460.
 98. Tsujimoto Y and Croce CM (1986) Analysis of the structure, transcripts, and protein products of *bcl-2*, the gene involved in human follicular lymphoma. *Proc Natl Acad Sci USA* **83**: 5214–5218.
 99. Belka C and Budach W (2002) Anti-apoptotic *Bcl-2* proteins: structure, function and relevance for radiation biology. *Int J Radiat Biol* **78**: 643–658.
 100. Wang S, Yang D and Lippman ME (2003) Targeting *Bcl-2* and *Bcl-X_L* with nonpeptidic small-molecule antagonists. *Semin Oncol* **30**: 133–142.
 101. Yip KW and Reed JC (2008) *Bcl-2* family proteins and cancer. *Oncogene* **27**: 6398–6406.
 102. Hara T, *et al* (2005) *Bcl-2* inhibitors potentiate the cytotoxic effects of radiation in *Bcl-2* overexpressing radioresistant tumor cells. *Int J Radiat Oncol Biol Phys* **61**: 517–528.
 103. Shiraiwa N, Okano H and Miura M (1997) *Bcl-2* prevents TNF- and Fas-induced cell death but does not inhibit initial processing of caspase-3. *Biomed Res* **18**: 405–411.
 104. Brosh R and Rotter V (2009) When mutants gain new powers: news from the mutant *p53* field. *Nat Rev Cancer* **9**: 701–713.
 105. Wang JL, *et al* (2000) Structure-based discovery of an organic compound that binds *Bcl-2* protein and induces apoptosis of tumor cells. *Proc Natl Acad Sci USA* **97**: 7124–7129.
 106. Manero F, *et al* (2006) The small organic compound HA14-1 prevents *Bcl-2* interaction with *Bax* to sensitize malignant glioma cells to induction of cell death. *Cancer Res* **66**: 2757–2764.
 107. An J, *et al* (2007) Overcoming the radioresistance of prostate cancer cells with a novel *Bcl-2* inhibitor. *Oncogene* **26**: 652–661.
 108. Kaplan HS and Murphy ED (1949) The effect of local roentgen irradiation on the biological behavior of a transplantable mouse carcinoma; increased frequency of pulmonary metastasis. *J Natl Cancer Inst* **9**: 407–413.
 109. von Essen CF (1991) Radiation enhancement of metastasis: a review. *Clin Exp Metastasis* **9**: 77–104.
 110. Wild-Bode C, *et al* (2001) Sublethal irradiation promotes migration and invasiveness of glioma cells: implications for radiotherapy of human glioblastoma. *Cancer Res* **61**: 2744–2750.
 111. Qian LW, *et al* (2002) Radiation-induced increase in invasive potential of human pancreatic cancer cells and its blockade by a matrix metalloproteinase inhibitor, CGS27023. *Clin Cancer Res* **8**: 1223–1227.
 112. Hynes RO (1992) Integrins: versatility, modulation, and signaling in cell adhesion. *Cell* **69**: 11–25.
 113. Giancotti FG and Ruoslahti E (1999) Integrin signaling. *Science* **285**: 1028–1032.
 114. Ruoslahti E (1992) The Walter Herbert Lecture. Control of cell motility and tumour invasion by extracellular matrix interactions. *Br J Cancer* **66**: 239–242.
 115. Friedlander DR, *et al* (1996) Migration of brain tumor cells on extracellular matrix proteins *in vitro* correlates with tumor type and grade and involves αV and β1 integrins. *Cancer Res* **56**: 1939–1947.
 116. Qian LW, *et al* (2003) Radiation stimulates HGF receptor/*c-Met* expression that leads to amplifying cellular response to HGF stimulation via upregulated receptor tyrosine phosphorylation and MAP kinase activity in pancreatic cancer cells. *Int J Cancer* **104**: 542–549.
 117. Jadhav U and Mohanam S (2006) Response of neuroblastoma cells to ionizing radiation: modulation of *in vitro* invasiveness and angiogenesis of human microvascular endothelial cells. *Int J Oncol* **29**: 1525–1531.
 118. Ohuchida K, *et al* (2004) Radiation to stromal fibroblasts increases invasiveness of pancreatic cancer cells through tumor-stromal interactions. *Cancer Res* **64**: 3215–3222.
 119. Paquette B, *et al* (2007) *In vitro* irradiation of basement membrane enhances the invasiveness of breast cancer cells. *Br J Cancer* **97**: 1505–1512.

120. Akino Y, *et al* (2009) Carbon-ion beam irradiation effectively suppresses migration and invasion of human non-small-cell lung cancer cells. *Int J Radiat Oncol Biol Phys* **75**: 475–481.
121. Goetze K, *et al* (2007) The impact of conventional and heavy ion irradiation on tumor cell migration *in vitro*. *Int J Radiat Biol* **83**: 889–896.
122. Folkman J (1971) Tumor angiogenesis: therapeutic implications. *N Engl J Med* **285**: 1182–1186.
123. Sonveaux P, *et al* (2003) Irradiation-induced angiogenesis through the up-regulation of the nitric oxide pathway: implications for tumor radiotherapy. *Cancer Res* **63**: 1012–1019.
124. Abdollahi A, *et al* (2003) SU5416 and SU6668 attenuate the angiogenic effects of radiation-induced tumor cell growth factor production and amplify the direct anti-endothelial action of radiation *in vitro*. *Cancer Res* **63**: 3755–3763.
125. O'Reilly MS, *et al* (1994) Angiostatin: a novel angiogenesis inhibitor that mediates the suppression of metastases by a Lewis lung carcinoma. *Cell* **79**: 315–328.
126. Camphausen K, *et al* (2001) Radiation therapy to a primary tumor accelerates metastatic growth in mice. *Cancer Res* **61**: 2207–2211.
127. Wachsberger PR, *et al* (2005) Effect of the tumor vascular-damaging agent, ZD6126, on the radioresponse of U87 glioblastoma. *Clin Cancer Res* **11**: 835–842.
128. Wachsberger P, Burd R and Dicker AP (2003) Tumor response to ionizing radiation combined with antiangiogenesis or vascular targeting agents: exploring mechanisms of interaction. *Clin Cancer Res* **9**: 1957–1971.
129. Jain RK (2005) Normalization of tumor vasculature: an emerging concept in antiangiogenic therapy. *Science* **307**: 58–62.
130. Preston DL, *et al* (2007) Solid cancer incidence in atomic bomb survivors: 1958–1998. *Radiat Res* **168**: 1–64.
131. Preston DL, *et al* (2002) Radiation effects on breast cancer risk: a pooled analysis of eight cohorts. *Radiat Res* **158**: 220–235.
132. Shellabarger CJ, Chmelevsky D and Kellerer AM (1980) Induction of mammary neoplasms in the Sprague-Dawley rat by 430 keV neutrons and X-rays. *J Natl Cancer Inst* **64**: 821–833.
133. Broerse JJ, *et al* (1982) Mammary carcinogenesis in different rat strains after single and fractionated irradiations. In *Neutron Carcinogenesis*, (Eds) Broerse JJ, Gerber GB, pp. 155–168. Commission of the European Communities, Luxembourg.
134. Imaoka T, *et al* (2009) Radiation-induced mammary carcinogenesis in rodent models: what's different from chemical carcinogenesis? *J Radiat Res* **50**: 281–293.
135. Shellabarger CJ, *et al* (1985) Neon-20 ion- and X-ray-induced mammary carcinogenesis in female rats. *Ann N Y Acad Sci* **459**: 239–244.
136. Dicello JF, *et al* (2004) *In vivo* mammary tumorigenesis in the Sprague-Dawley rat and microdosimetric correlates. *Phys Med Biol* **49**: 3817–3830.
137. Imaoka T, *et al* (2007) High relative biologic effectiveness of carbon ion radiation on induction of rat mammary carcinoma and its lack of H-ras and Tp53 mutations. *Int J Radiat Oncol Biol Phys* **69**: 194–203.
138. Nakadai T, *et al* (2004) HZE radiation effects for hereditary renal carcinomas. *Biol Sci Space* **18**: 177–178.
139. Ando K, *et al* (2005) Tumor induction in mice locally irradiated with carbon ions: a retrospective analysis. *J Radiat Res* **46**: 185–190.
140. Kakinuma S, *et al* (2004) Effect of carbon ions on life span shortening and tumorigenesis in mice. *Biol Sci Space* **18**: 190.
141. Watanabe H, *et al* (1998) Comparison of tumorigenesis between accelerated heavy ion and X-ray in B6C3F1 mice. *J Radiat Res* **39**: 93–100.
142. Watanabe H, *et al* (1998) Induction of ovarian tumors by heavy ion irradiation in B6C3F1 mice. *Oncol Rep* **5**: 1377–1380.
143. Durante M and Cucinotta FA (2008) Heavy ion carcinogenesis and human space exploration. *Nat Rev Cancer* **8**: 465–472.
144. Isaacs JT (1986) Genetic control of resistance to chemically induced mammary adenocarcinogenesis in the rat. *Cancer Res* **46**: 3958–3963.
145. Silverman J, *et al* (1980) Effect of dietary fat on X-ray-induced mammary cancer in Sprague-Dawley rats. *J Natl Cancer Inst* **64**: 631–634.
146. Shellabarger CJ (1972) Mammary neoplastic response of Lewis and Sprague-Dawley female rats to 7,12-dimethylbenz(a)anthracene or x-ray. *Cancer Res* **32**: 883–885.
147. Holtzman S, Stone JP and Shellabarger CJ (1981) Synergism of estrogens and X-rays in mammary carcinogenesis in female ACI rats. *J Natl Cancer Inst* **67**: 455–459.
148. Holtzman S, Stone JP and Shellabarger CJ (1979) Synergism of diethylstilbestrol and radiation in mammary carcinogenesis in female F344 rats. *J Natl Cancer Inst* **63**: 1071–1074.
149. Shellabarger CJ, Stone JP and Holtzman S (1978) Rat differences in mammary tumor induction with estrogen and neutron radiation. *J Natl Cancer Inst* **61**: 1505–1508.
150. Vogel HH Jr and Turner JE (1982) Genetic component in rat mammary carcinogenesis. *Radiat Res* **89**: 264–273.
151. Kumar R, Sukumar S and Barbacid M (1990) Activation of ras oncogenes preceding the onset of neoplasia. *Science* **248**: 1101–1104.
152. Imaoka T, *et al* (2008) Gene expression profiling distinguishes between spontaneous and radiation-induced rat mammary carcinomas. *J Radiat Res* **49**: 349–360.
153. Bettega D, *et al* (2009) Neoplastic transformation induced by carbon ions. *Int J Radiat Oncol Biol Phys* **73**: 861–868.
154. Imadome K, *et al* (2008) Upregulation of stress-response genes with cell cycle arrest induced by carbon ion irradiation in multiple murine tumors models. *Cancer Biol Ther* **7**: 208–217.
155. Tamaki T, *et al* (2009) Application of carbon-ion beams or γ -rays on primary tumors does not change the expression profiles of metastatic tumors in an *in vivo* murine model. *Int J Radiat Oncol Biol Phys* **74**: 210–218.

Received on November 20, 2009

Accepted on December 14, 2009

J-STAGE Advance Publication Date: ●●●, 2010

Long-term phlebotomy with low-iron diet therapy lowers risk of development of hepatocellular carcinoma from chronic hepatitis C

JUNJI KATO, KOJI MIYANISHI, MASAYOSHI KOBUNE, TOKIKO NAKAMURA, KOHICHI TAKADA, RISHU TAKIMOTO, YUTAKA KAWANO, SHO TAKAHASHI, MINORU TAKAHASHI, YASUSHI SATO, TETSUJI TAKAYAMA, and YOSHIRO NIITSU

Fourth Department of Internal Medicine, Sapporo Medical University School of Medicine, South-1, West-16, Chuo-ku, Sapporo 060-8543, Japan

Background. We have previously demonstrated that in patients with chronic hepatitis C (CHC), iron depletion improves serum alanine aminotransferase (ALT) levels as well as hepatic oxidative DNA damage. However, it has not been determined whether continuation of iron depletion therapy for CHC favorably influences its progression to hepatocellular carcinoma (HCC). **Methods.** We conducted a cohort study on biopsy-proven CHC patients with moderate or severe liver fibrosis who failed to respond to previous interferon (IFN) therapy or had conditions for which IFN is contradicted. Patients were divided into two groups: subjects in group A ($n = 35$) underwent weekly phlebotomy (200g) until they reached a state of mild iron deficiency, followed by monthly maintenance phlebotomy for 44–144 months (median, 107 months), and they were advised to consume a low-iron diet (5–7 mg iron/day); group B ($n = 40$) comprised CHC patients who declined to receive iron depletion therapy. **Results.** In group A, during the maintenance phase, serum ALT levels decreased to less than 60 IU/l in all patients and normalized (<40 IU/l) in 24 patients (69%), whereas in group B no spontaneous decrease in serum ALT occurred. Hepatocarcinogenesis rates in groups A and B were 5.7% and 17.5% at the end of the fifth year, and 8.6% and 39% in the tenth year, respectively. Multivariate analysis revealed that iron depletion therapy significantly lowered the risk of HCC (odds ratio, 0.57) compared with that of untreated patients ($P = 0.0337$). **Conclusions.** Long-term iron depletion for CHC patients is a promising modality for lowering the risk of progression to HCC.

Key words: chronic hepatitis C, phlebotomy, low-iron diet therapy, iron depletion therapy

Introduction

Hepatitis C virus (HCV) infection affects more than 170 million people worldwide and is a major cause of chronic hepatitis C (CHC), cirrhosis, and hepatocellular carcinoma (HCC) in most developed countries.^{1–3} Follow-up studies on the natural history of CHC over a mean period of 4–11 years have showed that cirrhosis develops in 8%–46% of cases and HCC in 11%–19%.^{2,4} At present, a combination of pegylated interferon (Peg-IFN) and ribavirin has been established as standard antiviral therapy for CHC.⁵ With this therapy, more than 80% of patients with HCV genotype 2 or 3 achieve a sustained virological response (SVR), but among patients with genotype 1, the most common type in many developed countries, including the United States, countries of northern Europe, and Japan, only 50% achieve SVR.^{3,6} In addition, IFN therapy is contraindicated in many patients because of complications such as uncontrolled depressive illness, autoimmune hepatitis, and poorly controlled diabetes.⁷ Accordingly, other approaches need to be pursued for managing patients who fail to respond to IFN therapy or for whom IFN therapy is not feasible. For such patients with CHC, therapeutic intervention to prevent or delay progression to lethal disease states, such as liver cirrhosis and HCC, are urgently needed.

Recent studies have shown that excess hepatic iron accumulation in CHC patients contributes to liver injury.^{8–10} Free iron in the liver is believed to facilitate the formation of reactive oxygen species (ROS), including hydroxyl radicals ($\cdot\text{OH}$), which cause oxidative damage of numerous cellular components such as lipids, proteins, and nucleic acids, and also upregulate collagen synthesis.¹¹ Further, the $\cdot\text{OH}$ radical is known to generate promutagenic bases such as 8-hydroxy-2-deoxyguanosine (8-OHdG), which has been implicated in spontaneous DNA mutagenesis and carcinogenesis.^{12,13} Although the mechanism of hepatocarcinogene-

Received: June 22, 2007 / Accepted: July 17, 2007

Reprint requests to: J. Kato

sis after HCV infection remains unclear, long-term follow-up studies indicate that most patients with progressive liver diseases who develop cirrhosis or HCC have persistently elevated or fluctuating serum alanine aminotransferase (ALT) levels, suggesting that they have a background of chronic active liver inflammation and regeneration.¹⁴ Hepatocellular damage from HCV infection may be initiated by various immunological reactions occurring on the cell surface, including interactions between Fas on hepatocytes and Fas ligand on cytotoxic T cells and between tumor necrosis factor (TNF) receptors on hepatocytes and TNF released from macrophages and other sources, which subsequently lead to apoptosis caused by $\cdot\text{OH}$ radicals generated in the presence of ferrous iron via a Fenton-type reaction.¹⁵ Thus, iron depletion of hepatocytes can theoretically prevent the generation of toxic ROS and may interfere with apoptotic signaling as well as oxidative DNA damage. In fact, we previously demonstrated that HCC can be completely prevented by a low-iron diet in LEC rats, which accumulate abnormally high levels of copper and iron in the liver and frequently develop HCC, suggesting that iron depletion is effective in decreasing oxidative DNA damage.¹⁶ Further, we also demonstrated in a 6-year follow-up study of CHC patients that iron depletion therapy, consisting of intermittent phlebotomies and a low-iron diet, significantly reduced serum ALT levels, the histological hepatic fibrosis grade, and hepatic 8-OHdG levels.¹⁰ However, it has not yet been determined whether continuation of iron depletion therapy for CHC can favorably influence the progression of disease to HCC.

Therefore, we conducted a cohort study of CHC patients with moderate to severe hepatic fibrosis (a population known to be at high risk for HCC) and examined whether iron depletion therapy could prevent progression to HCC. As a result, we here demonstrate that long-term iron depletion therapy for CHC patients is a promising modality for lowering the risk of progression to HCC.

Methods

Patients

The study enrolled 75 patients with biopsy-proven CHC who routinely visited the liver unit of our department between 1994 and 1996, and who met the following criteria: (1) adult (>20 years of age) with detectable anti-HCV antibodies and HCV-RNA; (2) previously treated with IFN therapy without achieving SVR or refusal/inability to receive IFN therapy; (3) persistently elevated serum ALT levels (>60 IU/l for >6 months) at least 1 year after IFN treatment; (4) histopathological evidence of chronic hepatitis with moderate to severe

grade liver fibrosis (F2 or F3) on liver biopsy; (5) negative test result for anti-nuclear antibody, anti-smooth muscle antibody, anti-mitochondrial antibody, and hepatitis B surface antigen; (6) no habitual drug or alcohol use; and (7) no administration of ursodeoxycholic acid or glycyrrhizin. The subjects consisted of 38 men and 37 women aged 34 to 75 years with a median age of 60 years. Patients with cirrhosis or a possible HCC association at the time of diagnosis of CHC were excluded from the study. Among the 75 patients, 35 (46.7%) received iron depletion therapy (iron depletion group) after providing written informed consent. The remaining 40 patients were those who declined to receive iron depletion therapy (control group).

Iron depletion therapy

Therapeutic iron depletion was accomplished by performing intermittent phlebotomies in combination with regulation of dietary iron intake as described previously.¹⁰ In brief, at the initial phase of iron depletion, all patients underwent a weekly phlebotomy of 200 g until a state of mild iron deficiency was achieved (defined by either by a serum ferritin concentration of <10 $\mu\text{g/l}$ or a blood hemoglobin concentration of 11.0 g/dl). The mild iron deficiency state was maintained by additional phlebotomies during the study period: patients were followed-up every 1 to 2 months for the duration of the study, and a phlebotomy (200 g) was performed if the hemoglobin level exceeded 11.0 g/dl. In addition, the iron depletion group subjects were instructed, both orally and in writing, by a registered dietitian (SK) to reduce their intake of iron-rich foods during the intervention. To aid with compliance, each subject was given a comprehensive list of iron-rich foods to avoid, and instructions on how to complete dietary records, which required the listing of all food and drink consumed over a 3-day period once every 3 months throughout the intervention. The subjects were not required to alter their total caloric intake, but they were expected to replace iron-rich foods with appropriate substitutes. All patients allocated to the low-iron diets were instructed to reduce their consumption of beans, shellfish, green vegetables, meat, and seaweed, and to replace them with refined carbohydrates. Dietary energy (1900–2000 kcal/day), nutritional balance and iron intake (5–7 mg/day) during the study period were assessed from the dietary records by using the nutrition analysis software Win Kenkoukun-III (Hokenjyouhou, Chiba, Japan).

Laboratory tests

Complete blood cell counts, iron levels (serum iron, serum ferritin, and transferrin saturation), and bio-

chemical parameters, including serum ALT, were determined by using automated procedures in the clinical laboratories of Sapporo Medical University Hospital at every visit. Serum HCV-RNA levels were determined by reverse transcriptase-polymerase chain reaction using a commercial kit (Amplicor HCV; Roche Diagnostics, Branchburg, NJ, USA), and HCV genotypes were assessed by the serological method with a commercial enzyme-linked immunosorbent assay kit (Kokusai Diagnostic, Kobe, Japan).

Liver biopsy

Liver biopsy obtained within 3 months of enrollment was required of all subjects. Biopsy specimens were formalin-fixed, stained with hematoxylin and eosin or Berlin blue, and reviewed by a single pathologist. Hepatic inflammation and fibrosis were scored by using the Knodell histological activity index.¹⁷ Hepatic iron staining was graded by the method of Barton et al.¹⁸

Follow-up of patients and diagnosis of HCC

Patients were followed up monthly by monitoring hematological and biochemical test results. Computed tomography or ultrasonography was performed every 3 or 4 months in all patients. Angiography was performed when HCC was highly suspected on the basis of computed tomography or ultrasonography imaging.

Statistical analyses

Nonparametric procedures, including the Mann-Whitney *U* test and the χ^2 -squared test, were employed for the analysis of background characteristics. The HCC incidence rate (hepatocarcinogenesis rate) was calculated, based on the period between the diagnosis of CHC by liver biopsy (control group) or start of iron depletion therapy (iron depletion group) and the appearance of HCC, using the Kaplan-Meier technique. Differences in the hepatocarcinogenesis curves were determined by using the log rank test. Independent factors associated with the incidence rate of HCC were analyzed by a stepwise Cox regression analysis. Although continuous variables without data conversion were used in the subsequent multivariate analyses, several variables were transformed into categorical data consisting of two simple ordinal numbers to obtain a hazard ratio. All factors found to be at least marginally associated with liver carcinogenesis ($P < 0.15$) were tested by the multivariate Cox proportional hazard model. $P < 0.05$ was considered to be significant. All data analysis was performed with the computer program SAS.

Results

Patient demographics

At the time of diagnosis of CHC, there were no significant differences between the iron depletion group ($n = 35$) and the control group ($n = 40$) in sex, age, history of blood transfusion, history of IFN therapy, serum albumin concentration, serum bilirubin concentration, serum ALT level, serum γ -glutamyl transpeptidase (GGTP) level, platelet count, serum α -fetoprotein (AFP) concentration, serum type IV collagen level, HCV serotype, HCV concentration, serum ferritin level, stage of liver fibrosis, or hepatic iron deposition score (Table 1). In the iron depletion group, 65.7% of patients had a serum ferritin value exceeding the normal range, and 60.0% in the control group. There was no significant difference between the two groups ($P = 0.779$). In the iron depletion group, Hb levels, serum iron, serum ferritin, and serum ALT levels at the end point were significantly decreased compared with the baseline levels (Table 2).

Crude rates of hepatocarcinogenesis

During the observation period of 144 months, HCC developed in 17/75 patients (22.7%); 4/35 (11.4%) in the iron depletion group, and 13/40 (32.5%) in the control group. As shown in Fig. 1, hepatocarcinogenesis rates in the iron depletion group and control group were 0% and 5.0% at the end of the third year, 5.7% and 17.5% at the end of the fifth year, and 11.8% and 39.0% at the end of tenth year. Log rank tests showed that the hepatocarcinogenesis rate in the iron depletion group was significantly lower than that in the control group ($P = 0.0182$).

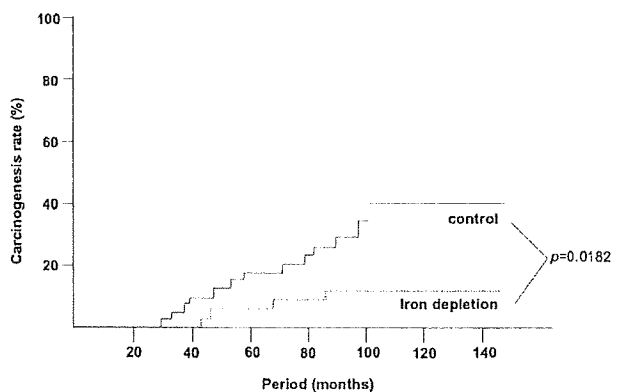


Fig. 1. Crude hepatocarcinogenesis rate in iron depletion and control groups. The carcinogenesis rate was significantly lower in the iron depletion group than in the control group (log rank test)